Exploring the phylogeny of the marattialean ferns

Samuli Lehtonen[a]*, Péter Poczai[b], Gaurav Sablok[b,c], Jaakko Hyvönen[b,c],
Dirk N. Karger[a,d] and Jorge Flores[b]

[a]*Biodiversity Unit, University of Turku, FI-20014, Turku, Finland;* [b]*Finnish Museum of Natural History (Botany), University of Helsinki, PO Box 7, FI-00014, Helsinki, Finland;* [c]*OEB and ViPS, University of Helsinki, PO Box 65, FI-00014, Helsinki, Finland;* [d]*Swiss Federal Research Institute, WSL, 8903, Birmensdorf, Switzerland*

Abstract

The eusporangiate marattialean ferns represent an ancient radiation with a rich fossil record but limited modern diversity in the tropics. The long evolutionary history without close extant relatives has confounded studies of the phylogenetic origin, rooting and timing of marattialean ferns. Here we present new complete plastid genomes of six marattialean species and compiled a plastid genome dataset representing all of the currently accepted marattialean genera. We further supplemented this dataset by compiling a large dataset of mitochondrial genes and a phenotypic data matrix covering both extant and extinct representatives of the lineage. Our phylogenomic and total-evidence analyses corroborated the postulated position of marattialean ferns as the sister to leptosporangiate ferns, and the position of *Danaea* as the sister to the remaining extant marattialean genera. However, our results provide new evidence that *Christensenia* is sister to *Marattia* and that *M. cicutifolia* actually belongs to *Eupodium*. The apparently highly reduced rate of molecular evolution in marattialean ferns provides a challenge for dating the key phylogenetic events with molecular clock approaches. We instead applied a parsimony-based total-evidence dating approach, which suggested a Triassic age for the extant crown group. The modern distribution can best be explained as mainly resulting from vicariance following the breakup of Pangaea and Gondwana. We resolved the fossil genera *Marattiopsis*, *Danaeopsis* and *Qasimia* as members of the monophyletic family Marattiaceae, and the Carboniferous genera *Sydneia* and *Radstockia* as the monophyletic sister of all other marattialean ferns.

© 2020 The Authors. *Cladistics* published by John Wiley & Sons Ltd on behalf of Willi Hennig Society.

Introduction

The eusporangiate fern order Marattiales represents a Palaeozoic radiation, currently comprised of ≈100 species in six genera (Murdock, 2008a; PPG I, 2016). Although their current distribution is restricted to the wet tropical regions (Murdock, 2008a; PPG I, 2016), a diverse fossil record has been found from all continents, including Antarctica (Stidd, 1974; Escapa et al., 2014). Due to its ancient origin and abundant fossil record, the phylogeny of the Marattiales has received considerable interest from both palaeontological and neontological perspectives (Mamay, 1950; Hill and Camus, 1986a; Hill and Camus, 1986b; Liu et al., 2000a; Christenhusz, 2007; Li and Lu, 2007; Christenhusz et al., 2008; Murdock, 2008b; Senterre et al., 2014; Cleal, 2015; Rothwell et al., 2018). Although the phylogenetic relationships of the early diverging fern lineages have remained ambiguous for a long time (Pryer et al., 2001; Wikström and Pryer, 2005; Rothwell and Nixon, 2006; Karol et al., 2010; Knie et al., 2015), the most recent studies based on phylogenomic data of plastomes (Grewe et al., 2013; Kim et al., 2014; Lu et al., 2015; Labiak and Karol, 2017; Gitzendanner et al., 2018; Kuo et al., 2018; Lehtonen, 2018; Lehtonen and Cárdenas, 2019) and transcriptome data (Rothfels et al., 2015; Qi et al., 2018; Shen et al., 2018) generally support a sister relationship between the marattialean and leptosporangiate ferns (but see Wickett et al., 2014, and One Thousand Plant Transcriptomes Initiative,

2019, for alternative resolutions). Based on the fossil record and molecular dating this split had occurred by the early Carboniferous with a rapid diversification until marattialean ferns reached their maximal diversity during the Palaeozoic (DiMichele and Phillips, 2002; Lehtonen et al., 2017). This was followed by extinctions at the Permo-Triassic boundary and the rise of more modern-appearing forms in the Mesozoic (DiMichele and Phillips, 2002; Lehtonen et al., 2017) with apparently continually diminishing ecological importance, as suggested by the almost complete lack of Cenozoic fossils (Collinson, 2001).

Marattiales generally is divided into two families: the now extinct Psaroniaceae (often called Asterothecaceae, see Cleal, 2015, for discussion about the correct name) and the extant Marattiaceae (Morgan, 1959). Psaroniaceae is a predominantly Palaeozoic family of mainly very large, arborescent ferns, which formed an important and sometimes dominant component of the coal swamp vegetation (Phillips et al., 1985; Millay, 1997; DiMichele and Phillips, 2002). Typical characteristics of Psaroniaceae include a massive, trunk-like stem with thick root mantle, highly divided large leaves with pecopteroid pinnule shape, and sporangia aggregated into radial synangia with limited fusion between the sporangia (Stidd, 1974; Millay, 1997). By contrast, Marattiaceae stems vary from slender and creeping, to large, fleshy and globular stems clothed with large stipules. Leaves are less divided with taeniopterid pinnules, and sporangia are generally fused into a bilaterally symmetrical synangia (Stidd, 1974; Hill and Camus, 1986a; Camus, 1990). Recently, Sydneideae, a new subfamily of Psaroniaceae was described for *Sydneia manleyi* Pšenička et al. with atypical sphenopteroid foliage and radially symmetrical synangia (Pšenička et al., 2014). The taxonomy of the fossil Marattiales has been studied extensively but is confounded by imperfect and variable preservation, making it difficult to reconstruct whole plants based on separately preserved stems, foliage fragments and reproductive structures (Lesnikowska, 1989), or to match permineralized material with adpression fossils (Cleal, 2015).

The taxonomic concepts of the extant Marattiaceae have varied over time, and the species-level taxonomy still remains disputed especially in the larger genera *Danaea* Sm. and *Angiopteris* Hoffm. (Christenhusz, 2007; Murdock, 2008a). The genus-level classification, however, was revised based on molecular studies by Murdock (2008a, b) and has since been accepted by authors (Christenhusz and Chase, 2014; Senterre et al., 2014; Arana, 2016; PPG I, 2016; Tuomisto et al., 2018). When compared with the older concepts, the most dramatic change was the splitting of the paraphyletic genus *Marattia* Sw. into three segregate genera: *Marattia*, *Eupodium* J.Sm. and *Ptisana* Murdock.

This classification is problematic from a palaeobotanical perspective, as numerous fossil species have been traditionally placed in the broadly defined *Marattia*, or *Marattiopsis* Schimp., a name that was established for those fossils that have generally similar morphological characteristics compared to extant species (Schimper, 1869). The problem is not only that the diagnostic morphological characters of the newly split genera are difficult to discern in fossil material, but also that many fossils seem to show a mixed set of these characters (Bomfleur et al., 2013; Escapa et al., 2014; Kvaček, 2014).

Given the ancient origin of the lineage, its lack of close extant relatives with the somewhat diffuse nature of the extant genera, and the presence of fossil material mixing the putative synapomorphies of the extant genera, it is not surprising that rooting the extant crown group Marattiaceae has remained problematic (Murdock, 2008b; Rothwell et al., 2018). Accordingly, this results in an uncertain interpretation of the character evolution and the biogeographical history of Marattiales. Although the marattialean phylogeny has been investigated quite widely, previous studies have either ignored the fossil evidence (Li and Lu, 2007; Christenhusz et al., 2008; Murdock, 2008b), or used very few if any molecular data from the extant species (Hill and Camus, 1986a; Liu et al., 2000a; Rothwell et al., 2018). The latest analyses (Li and Lu, 2007; Christenhusz et al., 2008; Murdock, 2008b; Senterre et al., 2014; Rothwell et al., 2018) have incorporated a good sampling of the extant species, but unfortunately included only a few molecular markers; hence, the potential of genomic characters has thus far not been exploited.

Over the past few years the number of completely sequenced fern plastomes has increased rapidly. Together with the transcriptome-based nuclear data, plastomes have been increasingly used to resolve challenging nodes of the fern phylogeny (Grewe et al., 2013; Kim et al., 2014; Lu et al., 2015; Labiak and Karol, 2017; Kuo et al., 2018; Lehtonen, 2018; Lehtonen and Cárdenas, 2019). At the same time, understanding of the structural evolution of the fern plastome has advanced greatly, leading to the emergence of a better view on how the ancestral genome structure has dynamically evolved through inversions, inverted repeat border expansions and contractions, and apparent insertions and deletions of mobile open reading frames (ORFs) into the plastome (Wolf et al., 2010; Gao et al., 2011; Grewe et al., 2013; Li et al., 2016; Robison et al., 2018; Lehtonen and Cárdenas, 2019). Marattialean ferns are of special interest in this context due to their phylogenetic position and apparent lack of RNA editing, a feature very common among the more derived ferns (Roper et al., 2007; Kim et al., 2014; Li et al., 2018). Thus, wider sampling

of marattialean plastomes, along with resolving their phylogenetic position and timing of origin, are of great interest for aiding the understanding of the evolution of fern plastid genome organization.

In this study, we generated a dataset of complete plastomes that represent all extant genera of Marattiaceae and compiled a phenotypic data matrix that represents all fairly well-known representatives of the marattialean ferns. Our data also allowed us to compile a large set of mitochondrial sequence data to be analyzed together with plastid and phenotypic characters. We then used these data to infer phylogenetic relationships and timing of diversification to investigate biogeographical hypotheses and explore the plastome genome evolution of this ancient fern order. We agree with Fitzhugh (2006) that there are no valid reasons to ignore any data that are potentially informative about phylogeny. As discussed by Wheeler et al. (2006), the commonly assumed distinction between genotypic and phenotypic data is artificial. We do acknowledge that there are real problems in combining all of the information in the same analyses, but this is not an excuse to ignore them, as the benefits obtained far outweigh the potential problems they cause. Studies that do not include known fossils implicitly treat them as separate from the phylogeny of extant organisms, which is an unrealistic stance.

Materials and methods

Taxon sampling

We aimed to investigate the phylogeny of marattialean ferns at two different levels. First, we explored their rooting and position within the overall fern phylogeny by analyzing a set of complete plastomes. Second, we further explored the marattialean rooting, phylogenetic resolution, and its timing by coding a taxonomically broad matrix of phenotypic characters from the representatives of extant and extinct marattialeans.

The extant marattialeans are currently classified into six genera (Murdock, 2008a; PPG I, 2016). We sampled the extant taxa at this level. Two complete marattialean plastomes were available in Gen-Bank (Roper et al., 2007; Zhu et al., 2015), both of them representing the genus *Angiopteris*. Thus, we extracted DNA from samples from the remaining four genera. The highest-quality extractions from each genus were selected for Illumina sequencing (see Molecular data below). However, the initial results indicated that our selected representative of the genus *Marattia* (*M. cicutifolia* Kaulf.) did not actually belong to *Marattia* but instead *Eupodium*, so we sampled another species from *Marattia*. Thus, we produced six new plastomes. Our final plastome data matrix consists of eight marattialean species that represent all six of the accepted genera. For the analysis of overall fern phylogeny, we complemented this sampling by downloading 16 additional fern plastomes from GenBank, widely representing the different fern lineages, and four seed plant plastomes for outgroup comparison (Table 1).

Furthermore, we compiled a phenotypic data matrix (see Phenotypic data below) for the eight marattialeans represented in the molecular data matrix. These were supplemented by coding data from 36 reasonably well-documented fossil marattialeans covering the taxonomic and temporal breadth of the lineage. We also added *Osmundastrum cinnamomeum* (L.) C.Presl (Osmundaceae) into this data matrix as an outgroup species. The osmundalean ferns are in several respects intermediate between the eusporangiate and leptosporangiate ferns, and have remained phenotypically (Phipps et al., 1998; Serbet and Rothwell, 1999) and perhaps also genetically (Bomfleur et al., 2014; Schneider et al., 2015) largely unmodified for extensive periods of time. Therefore, they are likely the most suitable extant outgroup for the marattialeans.

Molecular data

The total genomic DNA was extracted from silica dried material using either DNeasy Plant Mini Kit (Qiagen, Valencia, California, USA), E.Z.N.A. SP plant DNA kit (Omega Bio-tek, Doraville, Georgia, USA), or Macherey-Nagel NucleoSpin Plant II kit (Thermo Fisher Scientific, Waltham, Massachusetts, USA). DNA concentrations were determined with a Qubit fluorometer (Thermo Fisher Scientific,) and concentrated or diluted to $c.10$ ng/μL for library preparation. Paired-end 101-bp reads with a $c.300$-bp insert size were sequenced by Illumina HiSeq 2500 Sequencing System at FIMM Technology Center, Finland.

The produced reads were assembled into contigs by mapping them to the available *Angiopteris* plastomes and *de novo* using GETORGANELLE (Jin et al., 2018), NOVOPLASTY v.2.6.3 (Dierckxsens et al., 2016), VELVET v.1.2.08 (Zerbino and Birney, 2008), and GENEIOUS v.9.1.8 (www.geneious.com). The contigs thus obtained were then *de novo* assembled in GENEIOUS and the reads were mapped to the assemblies for verification and manual correction. Some gaps remained in the plastomes of *Ptisana novoguineensis* (Rosenst.) Murdock, *Eupodium kaulfussii* (J.Sm.) J.Sm. and *Marattia laxa* Kunze; and these were filled with Sanger sequencing using custom-designed primers (Table S1). The complete plastomes were annotated in GENEIOUS by comparing the initial annotations obtained in Dual Organeller GenoME Annotator (DOGMA; Wyman et al., 2004) with annotations on published sequences and ORFs.

Plastome coverage was evaluated in SAMTOOLS (Li et al., 2009) and BEDTOOLS (Quinlan and Hall, 2010) under the *genomecov* function by remapping the sequenced reads to the respective plastomes. To assess the synteny of the newly sequenced plastomes with the published ones we aligned the genomes with LASTZ (Harris, 2007) and MUMMER v.3.1 (Kurtz et al., 2004). Plastome coverage, gene tracks and synteny alignments were visualized with CIRCOS (Krzywinski et al., 2009) and GGBIO (Yin et al., 2012). A custom database was set up from the annotated plastid genomes in GENEIOUS, which was used to search previously described Mobile Open Reading Frames in Fern Organelles (MORFFO; Robison et al., 2018) using the default settings in TBLASTN (Altschul et al., 1990).

We performed a comparative analysis of simple sequence repeats using MISA by evaluating both simple as well as compound repeats (Thiel et al., 2003; Beier et al., 2017). MISA was used to analyze the perfect microsatellites often abbreviated as simple sequence repeats (SSRs) with a defined length of $n = 10$ in the case of mono-, $n = 6$ in the case of di-, and $n = 3$ in the case of tri-, tetra-, penta- and hexa-nucleotide repeats. For the compound repeats, two defined SSRs should be interrupted by 100 bp. Microstructural events such as inversions and single nucleotide polymorphism (SNP) (including deletions and substitutions) were identified using the pairwise alignments in LASTZ and MUMMER. Following the alignments, the show-snps feature in MUMMER along with the mummer plot was used for the identification of the plastome-wide and gene-wise plastomic variations.

We also produced a mitochondrial DNA (mtDNA) matrix by first mapping the reads of *Danaea sellowiana* C.Presl, the sample that had

Table 1
The plastome data used in this study

Taxon	Accession code	Reference
Adiantum capillus-veneris L.	NC_004766	Wolf et al. (2003)
Alsophila spinulosa (Hook.) R.M.Tryon	NC_012818	Gao et al. (2009)
Angiopteris angustifolia C.Presl	NC_026300	Zhu et al. (2015)
Angiopteris evecta (Forst.) Hoffm.	NC_008829	Roper et al. (2007)
Christensenia aesculifolia (Blume) Maxon	MN412587	This study
Cycas panzhihuaensis L.Zhou & S.Y.Yang	NC_031413	Han et al. (2017)
Cycas revoluta Bedd.	NC_020319	Li et al., unpublished
Cycas taitungensis C.F.Shen et al.	NC_009618	Wu et al. (2007)
Cyrtomium devexiscapulae (Koidz.) Ching	NC_028542	Lu et al. (2015)
Cyrtomium falcatum (L.f.) C.Presl	NC_028705	Choi and Park, unpublished
Danaea sellowiana Presl	MN412588	This study
Diplopterygium glaucum (Thunb. ex. Houtt.) Nakai	NC_024158	Kim et al. (2014)
Eupodium cicutifolium (Kaulf.) Lehtonen	MN412590	This study
Eupodium kaulfussii (J.Sm.) J.Sm.	MN412589	This study
Equisetum arvense L.	NC_014699	Karol et al. (2010)
Equisetum hyemale L.	NC_020146	Grewe et al. (2013)
Ginkgo biloba L.	NC_016986	Li et al., unpublished
Lygodium japonicum (Thunb.) Sw.	NC_022136	Gao et al. (2013)
Mankyua chejuensis B.Y.Sun et al.	NC_017006	Kim and Kim (2018)
Marattia laxa Kunze	MN412591	This study
Marsilea crenata C.Presl	NC_022137	Gao et al. (2013)
Myriopteris lindheimeri J.Sm.	NC_014592	Wolf et al. (2011)
Ophioglossum californicum Prant	NC_020147	Grewe et al. (2013)
Osmundastrum cinnamomeum (L.) C.Presl	NC_024157	Kim et al. (2014)
Psilotum nudum (L.) P.Beauv.	NC_003386	Wakasugi et al., unpublished
Pteridium aquilinum (L.) Kuhn	NC_014348	Der (2010)
Ptisana novoguineensis (Rosenst.) Murdock	MN412592	This study
Woodwardia unigemmata (Makinoi) Nakai	NC_028543	Lu et al. (2015)

the highest coverage of cpDNA, to the complete mitochondrion of *Ophioglossum californicum* Prantl (Guo et al., 2016) in GENEIOUS. The generated contigs were adjusted manually and the reads re-mapped on them to verify the sequence accuracy. Altogether, 39 contigs covering in total 36 862 bp were produced. The reads from the other newly sequenced samples were then mapped on these contigs with manual editing and remapping for verification when needed. In addition, we downloaded the raw sequence reads of *Angiopteris evecta* (G.Forst.) Hoffm. and *O. cinnamomeum* made available by the 1KP-project (Matasci et al., 2014), and compiled the mtDNA data for these taxa in the same manner as above. The resulting mtDNA matrix included all the same marattialean taxa that were represented in the cpDNA matrix with the exception of *Angiopteris angustifolia* C.Presl, from which only the published plastome sequence (Zhu et al., 2015) was available to us.

Phenotypic data

Seventy-seven phenotypic characters were obtained largely from the literature and scored for the studied taxa (Appendix 1). Scoring was based mainly on literature review but was confirmed for most of the extant taxa by studying the collections deposited in the herbarium of the University of Turku (TUR; see Appendix 1). A total of 18 characters were parsimony-uninformative in the current data matrix but are still listed here as they would be informative for broader taxonomic sampling of Marattiaceae and Osmundaceae. The list of characters and their states can be found in the Appendix 2, and the scored data matrix in the Appendix 3. All of the data matrices and resulting trees are available at TreeBASE (S25298), and the phenotypic data at MorphoBank (P3655).

Analyses of the phylogenetic position of Marattiales

For comparative phylogenomic analysis, a matrix of both the fern plastomes and seed plant outgroups (Table S2) was constructed by extracting the genes *acc*D, *atp*A, *atp*B, *atp*E, *atp*H, *atp*I, *ccs*A, *cem*A, *chl*B, *chl*L, *chl*N, *inf*A, *mat*K, *ndh*C, *ndh*D, *ndh*E, *ndh*F, *ndh*G, *ndh*H, *ndh*I, *ndh*J, *ndh*K, *pet*A, *pet*G, *pet*L, *pet*N, *psa*A, *psa*B, *psa*C, *psa*I, *psa*J, *psb*B, *psb*C, *psb*D, *psb*E, *psb*F, *psb*H, *psb*I, *psb*J, *psb*K, *psb*L, *psb*M, *psb*N, *psb*T, *psb*Z, *rbc*L, *rpl*14, *rpl*20, *rpl*21, *rpl*22, *rpl*23, *rpl*33, *rpl*36, *rpo*A, *rpo*B, *rpo*C2, *rps*2, *rps*3, *rps*4, *rps*8, *rps*11, *rps*14, *rps*15, *rps*18, *rps*19, *ycf*4 and *ycf*12 (67 genes in total), and performing alignments of coding regions with MACSE (Ranwez et al., 2011). The alignments subsequently were masked for the internal stop codons following the frameshift alignment algorithm correction as implemented in MACSE, and trimmed using trimAl (Capella-Gutierrez et al., 2009). Finally, before the construction of the super-matrix, the presence of terminal stop codons was checked; if identified they were subsequently removed from the trimmed alignments. The final matrix was constructed using SEQUENCEMATRIX v.1.8 (Vaidya et al., 2011). The phylogeny was inferred using two different maximum-likelihood (ML) methods. First, we used IQTREE (Nguyen et al., 2015) with the approximate likelihood-ratio test (aLRT), Shimodaira–Hasegawa likelihood-ratio test (sh-LRT), Akaike information criterion (AIC) and Bayesian information criterion (BIC) using MODELFINDER (Kalyaanamoorthy et al., 2017). UFBOOT2 (Hoang et al., 2018) was used for ultrafast bootstrap (BS) calculation. The key idea behind UFBOOT is to keep trees encountered during the ML-tree search for the original sequence alignment and to use them to evaluate the tree likelihoods for the BS sequence alignment. UFBOOT provides relatively unbiased BS estimates under mild model

misspecifications and reduces computing time while achieving more unbiased branch supports than standard BS (Hoang et al., 2018). Second, we ran RAxML v.8.2.9 under the GTR-GAMMA and CAT models (Stamatakis, 2014).

We time-calibrated the plastome phylogeny with BEAST 1.10.1 (Suchard et al., 2018). We set a Yule tree prior to keep the model as simple as possible, even if the two-parameter birth–death model might have fitted the data better (Gernhard, 2008). Based on simulation studies it appears that the choice of tree prior has relatively little impact as long as the sequence data are informative (Sarver et al., 2019) and we use a high number of calibration priors. We set calibration priors for 11 nodes, including the root node, using exponential prior distributions with a hard minimum and a soft maximum (with 5% prior probability distribution exceeding the constraint) ages for the nodes other than the root node, for which we applied a uniform prior (Table 2). The exponential prior favors ages close to the hard minimum age, therefore unrealistically assuming that sampled fossils represent the earliest occurrences of their lineages. We alleviated this problem by using relatively old soft maximum age constraints to flatten the prior distribution. As minimum ages, we used the minimum age boundaries of the geological formations from which the relevant fossils were found by applying the timescale of Walker et al. (2018). For most of the nodes we followed the soft maximum age constraints justified by Lehtonen et al. (2017). For seed plants, we applied the same soft maximum age as for the ferns and euphyllophytes (root node); this was set as middle Silurian, following Hao and Xue (2013). The molecular rate varies greatly between the fern lineages (Korall et al., 2010; Rothfels and Schuett-pelz, 2013) and it has been shown that in such cases the random local clock (RLC) model (Drummond and Suchard, 2010) outper-forms other clock models (Crisp et al., 2014). We therefore applied the RLC model and ran 14 chains of 30×10^7 generations sampling every 5000 generations, using the computing facilities of the CSC - IT Center for Science Ltd (csc.fi).

For the time-calibration, the molecular data were divided by genes and a greedy search was performed in PARTITIONFINDER v.2.1.1 (Guindon et al., 2010; Lanfear et al., 2012, 2017) to determine the best partition strategy with associated substitution models under the Bayesian Information Criteria. This resulted in four character sets, three of which were assigned GTR + I + G and one with TVM + G model of evolution. Convergence of the runs and effective sample sizes were checked in TRACER v.1.7.1 (Rambaut et al., 2018) before combining them in LOGCOMBINER v.1.10.1 (Rambaut and Drum-mond, 2002–2018a) with a 25% burn-in. A maximum clade credibil-ity tree was reconstructed using TREEANNOTATOR v.1.10.1 (Rambaut and Drummond, 2002–2018b) and visualized using FIGTREE v.1.4.4 (Rambaut, 2006–2018). To investigate the possible deviation of spec-ified and effective calibration priors due to prior interactions (Heled and Drummond, 2011), we re-ran the analysis by sampling from the prior only.

Analyses of the phylogenetic relationships within Marattiales

The more detailed analyses on the marattialean relationships were performed for various data combinations to examine how the signal varies between pheno- and genotypic data, or if the inclusion of fos-sil terminals has a significant role in determining the topology. Hence, we separately analyzed cpDNA and mtDNA datasets and a phenotypic dataset including and excluding the fossils. We finally combined the datasets of all pheno- and genotypic characters includ-ing and excluding the fossils.

Tree searches under parsimony as optimality criterion were per-formed with TNT v.1.5 (Goloboff and Catalano, 2016) using 10 ini-tial replicates per hit. For each replicate, 20 iterations of Tree Drifting and Sectorial Searches were performed; five rounds of Tree Fusing subsequently were conducted to search for optimal trees (Goloboff, 1999). Searches were terminated after the best score was hit seven times. Support values were estimated with Symmetric Resampling, employing the difference between the most frequent groups and their most frequent contradictory group (GC; Goloboff, 2003).

The phylogenetic hypotheses were assessed for their sensitivity to the variation in the analysis parameters. In addition to equal weight-ing, the data were analyzed under extended implied weighting by using four different concavity values as reference ($k = 5$, $k = 10$, $k = 15$ and $k = 20$; Goloboff, 2014). In this set of analyses, individ-ual characters were weighted by considering the proportion of miss-ing entries, where each missing entry was assumed to have half of the homoplasy of the observed entries ($P = 0.5$). Although the entire range of weighting values were employed to evaluate sensitivity, $k = 15$ was arbitrarily selected as an intermediate concavity value (regarding $k = 5$ and equal weighting as the strongest and weakest weighting schemes, respectively) to further estimate nodal support, divergence times, and to be used as a reference for investigating the sensitivity.

In addition to the parsimony analyses, we analyzed the same data-sets using MRBAYES v.3.2.6 (Ronquist et al., 2012b) in CIPRES (Miller et al., 2010). The data partitioning and model selection were performed with PARTITIONFINDER (Lanfear et al., 2017) as indicated above. For the phenotypic dataset, we applied the Markov k model

Table 2
Node calibrations applied in the BEAST analysis

Clade	Stem/ crown	Fossil	Hard min age	Soft max age	Reference
Euphyllophyta	Stem	*Eophyllophyton*	407.6 Ma*	427.4 Ma*	Hao and Xue (2013)
Seed plants	Crown	Cordaitales	315.2 Ma	407.6 Ma	Falcon-Lang (2005)
Ferns[†]	Stem	*Ibyka*	382.7 Ma	407.6 Ma	Skog and Banks (1973)
Equisetales	Stem	*Archaeocalamites*	358.9 Ma	407.6 Ma	Stewart and Rothwell (1993)
Marattiales	Stem	*Psaronius*	323.2 Ma	407.6 Ma	Gerrienne et al. (1999)
Osmundales	Stem	*Grammatopteris*	272.95 Ma	358.9 Ma	Rößler and Galtier (2002)
Gleicheniales	Stem	*Chansitheca*	272.95 Ma	358.9 Ma	He et al. (2016)
Schizaeales	Stem	*Stachypteris*	168.3 Ma	298.9 Ma	Wikström et al. (2002)
Marsileaceae	Stem	*Marsileaceaephyllum*	139.8 Ma	201.3 Ma	Hu et al. (2008)
Pteridaceae	Stem	*Pteris*	93.9 Ma	201.3 Ma	Krassilov and Bacchia (2000)
Woodwardia	Stem	*Woodwardia*	56.0 Ma	145.0 Ma	Wang et al. (2006)

[*]Uniform prior.
[†]Monophyly enforced.

with only variable characters (Mkv) (Lewis, 2001). Both the cpDNA and mtDNA datasets were divided in four partitions when analyzed separately; in the combined analysis these data were divided in six partitions. Details about the data partitioning and model settings can be found in Appendix S1. For each data combination analyzed, two independent MrBayes runs, each comprising four chains, were conducted with sampling every 2000 generations. In total 2×10^7 generations were run for each analysis and the convergence was assessed in Tracer v.1.7.1 (Rambaut et al., 2018). All of the effective sample sizes were >500 after discarding the first 25% of the sample as burn-in.

Although tip-dating methods that include fossil data are available (Marjanović and Laurin, 2007; Ronquist et al., 2012a; Sterli et al., 2013; Grimm et al., 2015), they are relatively rarely used. Furthermore, the phylogenetic placement of fossils, which often is unstable, is seldom considered explicitly (Pyron, 2011). Our initial trials to tip-date the phylogeny with fossils in MrBayes were unsatisfactory due to poor convergence and great sensitivity to changes in prior settings. To provide an approximation of the divergence times within Marattiales, a parsimony-based method using the stratigraphic data associated with fossils (Sterli et al., 2013) was employed instead. This approach relies on both optimizing minimum ages of nodes and incorporating the phylogenetic uncertainty in placement of fossils by means of bootstrapping trees (Sterli et al., 2013). The optimization approach of the age character is derived from the metrics of phylogenetic stratigraphic fit (Siddall, 1996, 1998; Pol and Norell, 2001), whereby the transformation costs among character states are given by a symmetrical step matrix based on the absolute time difference between each state. Following Pol and Norell (2001), the transformation costs were set to be irreversible to an older age. Hence, allowing gaps in the stratigraphic data ("ghost lineages") to be taken into account (Pol et al., 2004). Divergence times then are approximated from the branch lengths after the optimization of this age character (Sterli et al., 2013). Depending on the completeness of the sampled fossil record, branches might be assigned zero lengths in this type of calibration methods (Wang and Lloyd, 2016). To avoid these artificial zero-length branches, they were "smoothed" by using a constant minimum branch length of 0.1. The impact of the fossil uncertain phylogenetic placement on the age estimates is captured in the Bootstrap Uncertainty Range (BUR); this is computed after calibrating the bootstrapping trees for both the maximum and minimum ages (BUR_{max}, BUR_{min}; Sterli et al., 2013). We followed Sterli et al. (2013) and disregarded the 2.5% of BS trees yielding the youngest (from the trees inferred during the BUR_{min} run) or oldest (from the trees inferred during the BUR_{max} run) ages. For the present study, divergence times were first calculated on the most parsimonious tree (s) obtained under $k = 15$. The divergence time uncertainty ranges subsequently were calculated from the bootstrapping trees recovered under the same concavity value. The maximum and minimum ages from the geological strata from which fossils are known were employed in the age range estimations (BUR_{max}, BUR_{min}). It should be noted that both BUR_{max} and BUR_{min} refer to minimum age estimations and the range, thus represent the uncertainty in minimum age estimation and not an uncertainty range of the node age (Sterli et al., 2013).

Biogeography

We analyzed the biogeographical history of Marattiales based on the parsimony-dated total-evidence phylogeny and by applying the dispersal-extinction-cladogenesis (DEC; Ree and Smith, 2008) model as implemented in R/biogeobears v.0.2.1 (Matzke, 2013a, b). We considered the following nine biogeographical regions in our analyses: Eurasia, Africa, Madagascar, India, Australia, North America, South America, Oceania and Antarctica. For *Marattia laxa* and *Ptisana novoguineensis*, we coded the geographical ranges of their respective genera in order to reconstruct the genus-level distribution patterns; in other extant taxa the species-level distributions covered the genus-level distributions. The application of genus ranges to species could be seen as a violation of the biogeographical model, but we consider this approach justified in our case. This is because despite the fact that many species of *Ptisana* are local endemics, some are quite widespread and are distributed almost throughout the range of the genus (Murdock, 2008a). *Marattia laxa*, however, covers the range of *Marattia* as here defined with the exception of Hawaii, where a very closely related *M. douglasii* is present (Murdock, 2008a). Furthermore, the natural range of the most widespread species in our analysis, *Angiopteris evecta*, covers multiple biogeographical regions and the whole range of its genus. Thus, in the absence of complete taxonomic sampling it seems reasonable to apply genus-level ranges for these taxa. For the fossil species we only coded the positive occurrences, and coded question marks for the regions from where they were not observed.

We constructed a time-stratified palaeographical model taking into account changes in continental plate positions for seven time intervals: 0–30, 30–50, 50–70, 70–90, 90–110, 110–180 and 180–350 Ma, following the plate tectonic model in Scotese (2016). We applied a different connectivity matrix for each time interval (Appendix S2) and set Antarctica as an area not allowed for the latest time interval when the continent has been glaciated (Carter et al., 2017). The area connectivity matrices were constructed so that a dispersal probability of 1.0 was assigned to all areas directly connected and a probability of 0.5 to areas that were either connected through another area(s) or were separated by a relatively narrow sea. A dispersal probability of 0.01 was assigned for areas separated by wide oceanic barriers and for Northern and Southern Hemisphere continents that were not directly connected in the Pangaea-configuration (e.g. dispersal probability of 1.0 from directly connected Australia to Antarctica, and 0.5 from Australia to indirectly connected South America, but 0.01 from Southern Hemisphere Australia to Northern Hemisphere Eurasia at 180–350 Ma).

Results

Plastome structure

We assembled and annotated six plastid genomes representing the Marattiaceae. High-throughput sequencing ranged from 15 922 in the case of *Ptisana novoguineensis* to 347 362 plastid genome reads for *Danaea sellowiana* (Table 3). Mapping of the reads to the *de novo* plastid genomes indicated that a mean coverage ranged from ×11 (*P. novoguineensis*) to ×240 (*D. sellowiana*) (see Fig. S1). Of the assembled plastomes, that of *D. sellowiana* was the smallest in size (145 892 bp), whereas *Eupodium kaulfussii* was the largest (151 986 bp). The genome structure of marattialean ferns showed similar quadripartite structure as in the seed plants, comprising a large-single copy (LSC), small-single copy (SSC) and two inverted repeat (IR) regions. Across Marattiaceae, gene content seems to be stable, with 86–87 protein-coding genes, 37 tRNA genes and four rRNA genes annotated in the genomes (Fig. 1). The distribution of these genes was similar to seed plants or other fern species, with 18 genes located in the SSC, 15 genes in the IRs and

90 genes in the LSC regions (Fig. S2). The overall GC content of the plastomes varied between 32.8 and 40.8%, whereas 29.5–31.2% of the whole genome was noncoding, which is congruent with previous reports (Robison et al., 2018). However, a lower GC content was observed for *E. cicutifolium* (32.8) and *E. kaulfussii* (32.8), reflecting different mutation/conversion biases in these genomes.

There were 18 intron-containing genes among Marattiaceae plastomes. Among these, 16 genes had a single intron (ten protein-coding and 6 tRNA), and two (*ycf*3, *clp*P) had two introns, whereas the *rpo*C1 intron has been lost from *D. sellowiana*. The loss of the same intron has been reported previously in Japanese climbing fern (*Lygodium japonicum*; Gao et al., 2013). The largest intron was the group II mitochondrial ORF-like intron of the *trn*K-UUU gene (2387–2427 bp) encompassing the variable *mat*K. The large gene *rps*12 appeared to be trans-spliced, with one exon located in the LSC and two exons in the IRs. We confirmed the presence of the *ycf*66 gene across Marattiaceae. This highly unstable gene has been lost independently at least four times, and has been pseudogenized in ferns (Gao et al., 2011). The adjacent *chl*L and *chl*N genes were located in the SSC region, creating an operon in the complete nucleotide sequences of marattialean ferns, whereas the *chl*B gene was disjunct in the LSC region. These three genes encode the subunits of the light-independent enzyme protochlorophyllide oxidoreductase required for chlorophyll formation in the dark. Their presence has been confirmed in the plastid genomes of at least some conifers, green algae and photosynthetic bacteria, but they are absent from major lineages of Poaceae and Solanaceae (Nazir and Khan, 2012). The *psbC/psbD* genes were the only overlapping genes among the plastid genomes. The partial overlap of these genes encoding the D2 and CP43 proteins of the photosystem II complex could be attributed to cotranscription. In *ccs*A, *rpo*B and *rps*15 genes, we observed the use of the alternative start codon ACG instead of the common AUG in *Marattia laxa*. Genes with such exceptional start codons are RNA edited in Asteraceae (Sablok et al., 2019) and Solanaceae (Amiryousefi et al., 2018). The diversity of RNA editing in ferns is somewhat unclear, as the abundant U-to-C edits are lacking in major lineages. There is evidence, however, for abundant C-to-U and U-to-C backedits in early diverging (*Equisetum* L., *Psilotum* Sw.) and in derived leptosporangiate ferns (*Adiantum* L., *Pteridium* Gled. ex Scop) (Guo et al., 2015; Li et al., 2018). RNA editing might be present in *M. laxa* but confirming this would require further transcriptomic data.

We searched for and characterized mobile elements collectively termed as MORFFO described from fern plastomes (Logacheva et al., 2017; Kim and Kim,

Table 3
Characteristics of the assembled plastomes

| Taxon	Voucher specimen	Number of reads	cpDNA reads	Average coverage	% mapping to plastome	Plastome size
Christensenia aesculifolia	*Walker, s.n.* (UC)	9 227 728	144 225	x 97	1.56%	149 900
Danaea sellowiana	*M.ynssen 1074* (TUR)	32 115 232	347 362	x 240	1.08%	145 892
Eupodium cicutifolium	*Christenhusz 4781* (TUR)	49 350 076	99 658	x 67	0.20%	151 257
Eupodium kaulfussii	*Lehtonen 571* (TUR)	34 092 632	228 912	x 152	0.67%	151 986
Marattia laxa	*Christenhusz 1313* (TUR)	33 251 026	60 819	x 42	0.18%	147 024
Ptisana novoguineensis	*Karger 1721* (Z)	23 920 596	15 922	x 11	0.07%	148 722
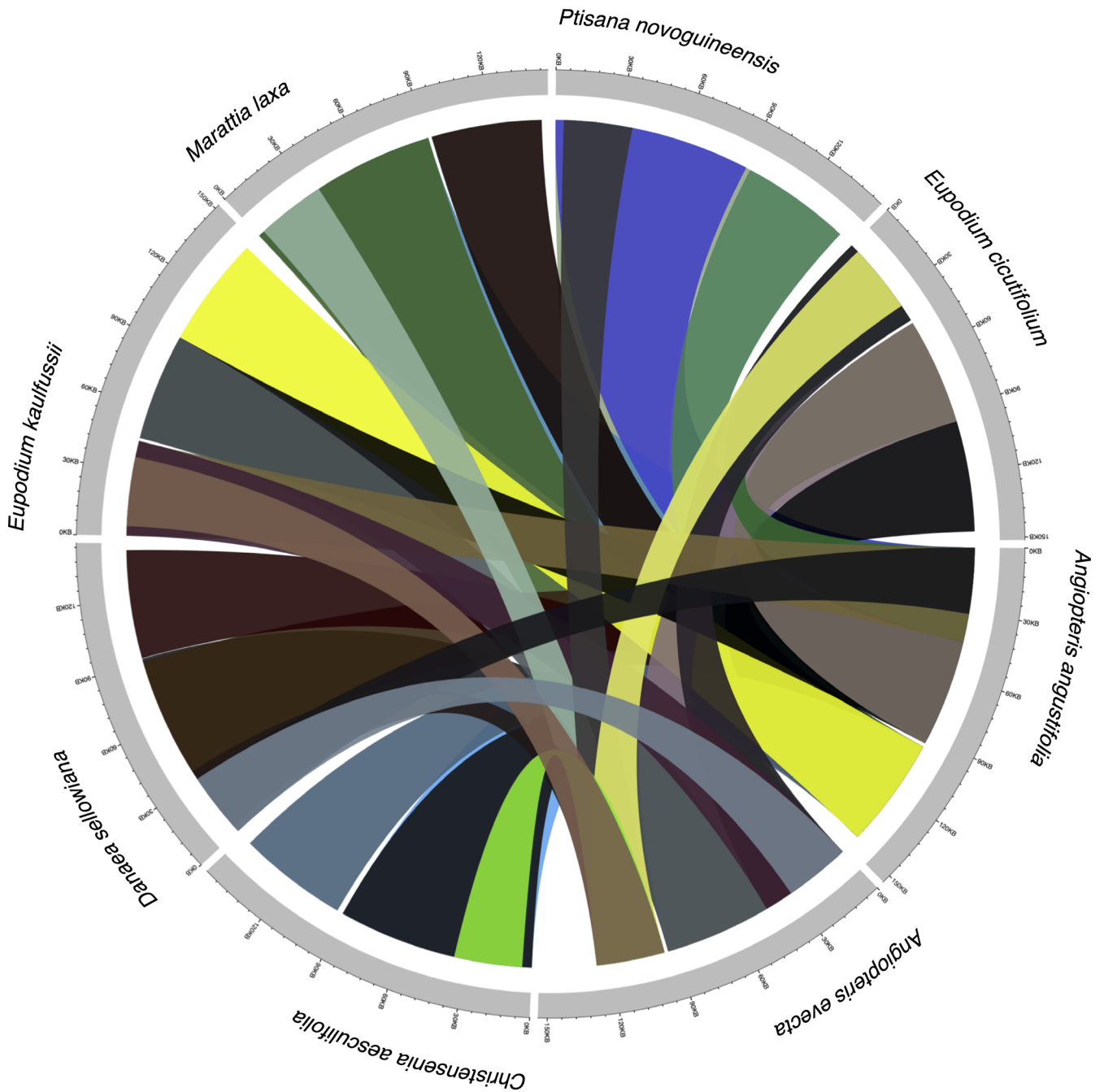
Fig. 1. Syntenic visualization of the Marattiaceae plastomes showing a generally conserved structure. Whole-genome plastome alignment using LASTZ and visualization using CIRCOS

2018; Robison et al., 2018; Lehtonen and Cárdenas, 2019). Our analysis indicated the absence of MORFFO elements in Marattiaceae except for the following cases: fractions of MORFFO1 were found between *trn*T and *trnf*M in *Eupodium cicutifolium* and *E. kaulfussii*, MORFFO2 between *trn*L and *ndh*B in *Angiopteris evecta*, and MORFFO3 element between *trn*L and *ndh*B in *Christensenia aesculifolia*,

respectively. The MORFFO1 hit in *Eupodium* overlapped with a 936-bp-long ORF. Likewise, we found an uninterrupted ORF of >1300 bp located between *trn*L and *ndh*B in *Christensenia* and in both *Angiopteris* species. Accordingly, our BLAST search matched the MORFFO3 at the 5' end of this ORF in *C. aesculifolia* and MORFFO2 at the 3' end of the ORF in the same genomic position in *A. evecta*. No match was

found to the ORF at this position in *A. angustifolia*, and in other species no uninterrupted ORFs of significant length were found at this position. We further queried the translated amino acid sequences of these ORFs against the NCBI protein database using Blastp (Altschul et al., 1990). The >1300-bp-long ORF in *C. aesculifolia*, *A. evecta* and *A. angustifolia* all matched with the annotated ORF531 in the *Mankyua chejuensis* B.Y.Sun et al. plastome (KP205433; Kim and Kim, 2018). The 936-bp-long ORF in *Eupodium* matched with the annotated ORF295 in the *Mankyua* B.Y.Sun et al. plastome.

Broad-scale phylogeny and node calibration

The plastomes of Marattiaceae and other ferns were analyzed under ML and node-calibrated with Bayesian inference. All of these analyses resulted in the same tree topology (Fig. 2). *Equisetum* was resolved as the sister to Ophioglossidae with a low support value (PP = 0.62, BS = 72), and Marattiaceae as the sister to leptosporangiate ferns (PP = 0.80, BS = 100). The family Dennstaedtiaceae, represented by *Pteridium* in our analyses, was resolved as diverging earlier than Pteridaceae, represented by *Adiantum* and *Myriopteris* Fée, albeit with a low posterior probability (PP = 0.95) and no BS value. The relative phylogenetic positions of Dennstaedtiaceae and Pteridaceae have remained notoriously difficult to resolve (e.g. Schuettpelz and Pryer, 2007; Lehtonen, 2011; Rothfels et al., 2015; Qi et al., 2018; Shen et al., 2018; Lehtonen and Cárdenas, 2019). Within Marattiaceae, *Danaea* was resolved as the sister to the remaining taxa in all the analyses, but not with maximum support value (PP = 0.97, BS = 94). *Marattia cicutifolia* was sister to *Eupodium kaulfussii* with maximum support value, whereas *M. laxa* was resolved in a distinct position as sister to *Christensenia*, but without maximum support value (PP = 0.89, BS = 94). The *Christensenia-M. laxa* clade was sister to *Angiopteris*, and these together formed a sister clade to the *Ptisana-Eupodium-M. cicutifolia* clade.

Divergence time analysis using BEAST did not converge well, as can be seen from the trace plot (Fig. 2). The effective sample size (ESS) values were >145 for each parameter. In the maximum clade credibility tree, ferns diverged from the seed plants at 420 Ma (95% CI: 409–427) and the fern crown group diverged at 388 Ma (95% CI: 359–420). Marattiales originated at 373 Ma (95% CI: 343–408), and the deepest divergence within extant species was dated at 61 Ma (95% CI: 47–108). The deepest divergence within the leptosporangiate ferns was dated at 330 Ma (95% CI: 311–347). In most cases the specified priors, as they were set up, closely matched the effective prior distributions as observed through running the analysis without data (Fig. 2). This was not the case with the seed plant prior, and even less so with the Marattiales prior, where the exponential prior was set up with an offset at 323.3 Ma, but the effective prior peaked at 410 Ma.

Marattialean phylogeny and parsimony dating

The phylogenetic relationships within Marattiales were analyzed in more detail by expanding the plastome data with mtDNA and morphology; the latter data also coded for selected fossil terminals. Analyses of these data under Bayesian inference and parsimony resulted in largely congruent topologies (Fig. 3). Implied weighting in parsimony analyses did not change the topologies except for the analyses including fossils, in which case the resolution—and to some degree the topology—varied depending on the *k*-value. The parsimony analysis of phenotypic data including only extant taxa resolved *Danaea* as the first diverging lineage within Marattiaceae, followed by *Christensenia*. The remaining species formed a clade with the two species of *Angiopteris* resolved as sisters, as were *E. kaulfussii* and *M. cicutifolia*; *M. laxa* and *P. novoguineensis* remained unresolved within this clade. The topology remained the same across all the *k*-values. The Bayesian analysis resulted in basically the same topology, but with *P. novoguineensis* and *M. laxa* resolved as successively diverging lineages on the branch leading to *Angiopteris*.

The topological arrangements within the extant species slightly changed when the extinct taxa were included in the analysis. In parsimony analyses, the positions of *M. laxa* and *P. novoguineensis* somewhat varied under equal weighting and *k* = 5, but with higher *k*-values they were constantly resolved as successively diverging lineages on the branch leading to *Angiopteris*. In the Bayesian analysis the inclusion of fossil taxa made *Danaea* and *Christensenia* sisters and collapsed *P. novoguineensis* and *M. laxa* to the same position as in parsimony analysis of extant taxa only. Beyond the extant species, the limited resolution present in Bayesian and equally weighted parsimony trees was largely congruent. In both trees, *Qasimia* Hill et al. (with two species) was sister to the clade that included all the extant Marattiaceae. The Bayesian analysis also resolved *Danaeopsis* Heer ex Schimp. (with three species, one of them missing a nomenclatural combination in *Danaeopsis*) within this clade. The fossil taxon *Marattiopsis vodrazkae* Kvaček was quite consistently resolved as sister to the extant *Eupodium kaulfussii*, except only in parsimony analysis with *k* = 5. The remaining species of *Marattiopsis* were somewhat unstable, although constantly placed within the same clade with the extant
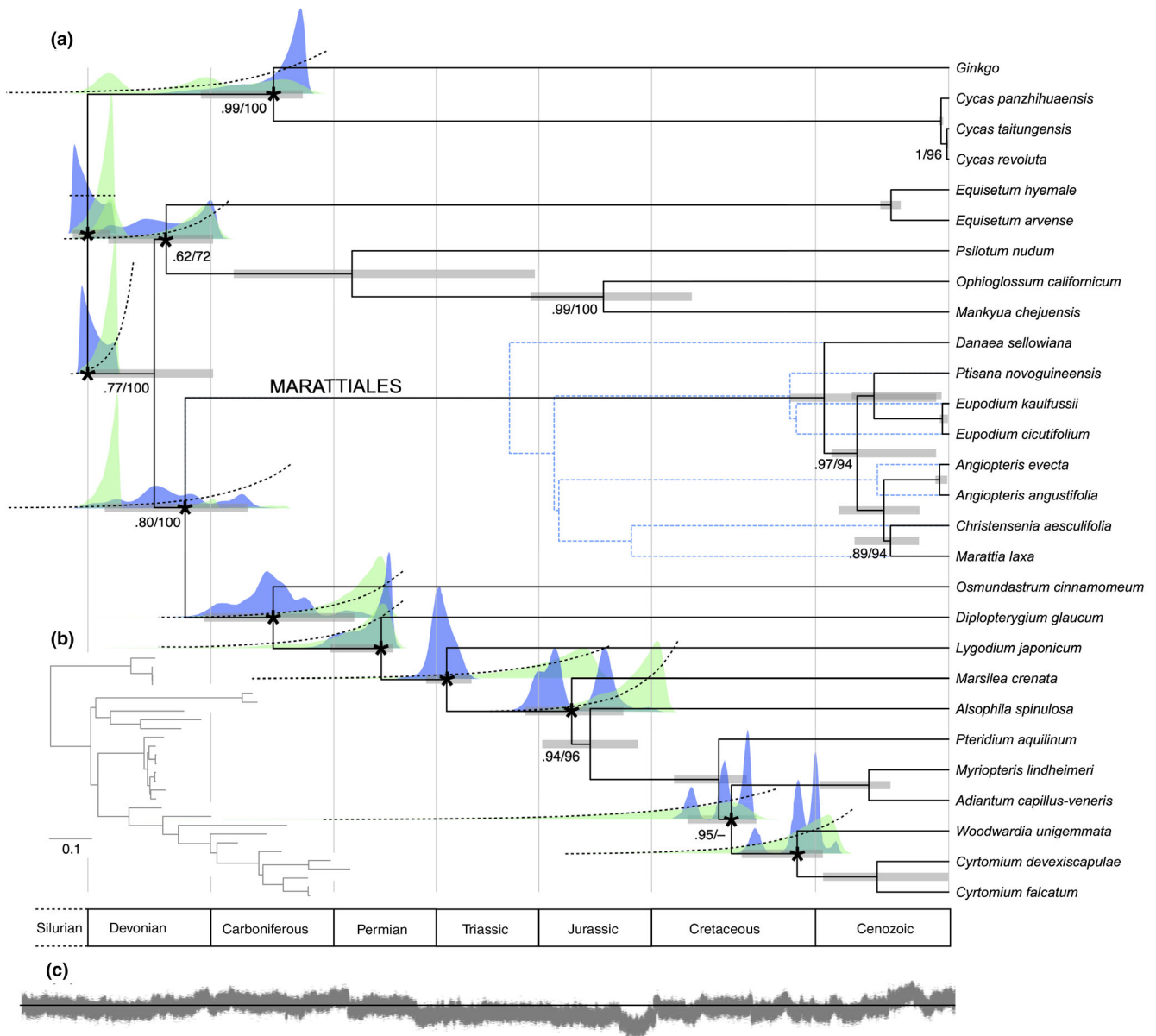
Fig. 2. Plastome phylogeny of ferns and seed plant outgroup. (a) Node-calibrated Bayesian maximum clade credibility tree with 95% HPD interval for node ages presented in horizontal bars. Asterisks denote calibrated nodes, specified calibration priors are shown with dotted lines, density distributions sampled from prior only (effective priors) are shown for these nodes in green, and posterior density distributions in blue. Nodal support values (Bayesian PP/ML bootstrap) are shown if not maximally supported. For the marattialean ferns, the tree dated with parsimony bootstrapping (see Fig. 4) is shown in the background with blue dotted lines. (b) The ML tree for the same plastome data. (c) Post-burn-in likelihood traces of the 14 chains are combined to show the sampled joint probability and the poor convergence of the chains. A horizontal line is provided for illustrative purposes

Marattiaceae. *Angiopteris blackii* Van Cittert, another fossil taxon, constantly formed a clade with the extant *Angiopteris*. The Bayesian analyses and all of the parsimony analyses, except the equally weighted analysis, resolved *Sydneia* Pšenička et al. and *Radstockia* Kidston as a clade sister to the remaining Marattiales. Psaroniaceae mostly remained unresolved in the Bayesian and equally weighted parsimony

analyses, but under implied weighting this extinct family was almost constantly resolved as sister to Marattiaceae (with *Sydneia* and *Radstockia* as a sister clade to the Psaroniaceae-Marattiaceae clade). The relationships within Psaroniaceae varied depending on the *k*-value, but *Danaeites* Goeppert and *Millaya* Mapes & Schabilion formed a sister clade to the remaining family almost constantly.
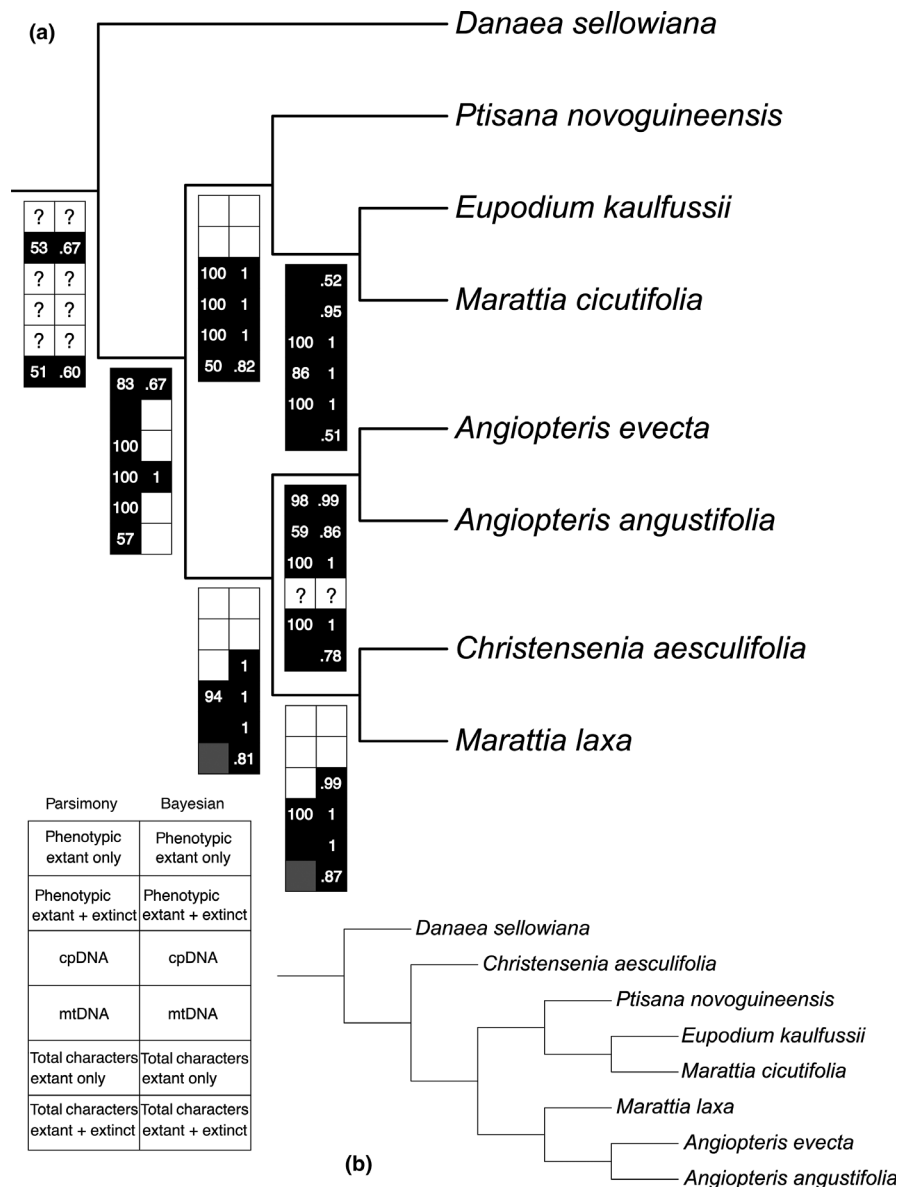
Fig. 3. Alternative hypotheses of the phylogenetic relationships of extant Marattiaceae. (a) Sensitivity of the most commonly obtained topology under different datasets in parsimony and Bayesian analyses. Black boxes indicate monophyly of the node under the indicated analysis, grey boxes indicate that monophyly was obtained with all implied weights but not in the equal weighted analysis. (b) Alternative topology obtained in the parsimony analyses of cpDNA and phenotypic data. Numbers indicate symmetrical resampling/posterior probability values >50%

The plastome data resulted in somewhat different topologies depending on the optimality criterion. Parsimony analysis resolved *Danaea* and *Christensenia* as successive lineages leading to the remaining Marattiaceae with maximum support value, *Ptisana* with maximum support value as sister to the *E. kaulfussii-M. cicutifolia* clade and *M. laxa* as sister to *Angiopteris*, albeit without support value. By contrast, the Bayesian analysis resolved *Christensenia* as sister to *M. laxa* (PP = 0.99), and these together as sister to *Angiopteris* (PP = 1). *Danaea* was sister (PP = 1) to a

clade where *Ptisana* was sister (PP = 1) to the *E. kaulfussii-M. cicutifolia* clade (PP = 1).

The mtDNA analyses resulted in congruent topologies with high support values across all the analyses. *Danaea* was resolved as the sister to the remaining Marattiaceae, *Christensenia* as sister to *M. laxa*, and these together as sister to *Angiopteris*; this clade was sister to a clade in which *Ptisana* was sister to the *E. kaulfussii-M. cicutifolia* clade.

The parsimony analysis of phenotypic and DNA data of extant taxa only resulted in the same topology

as mtDNA but with decreased support value for the sister relationships between the *Christensenia-M. laxa* clade and the sister relationships of this clade to *Angiopteris*. Bayesian analysis resulted in the same topology as the plastome data with *Danaea* as sister to the *Ptisana-Eupodium* clade (PP = 1).

In the total-evidence analyses (fossils included), the extinct *Angiopteris blackii* was resolved as sister to the extant *Angiopteris*, and this clade was sister to the *Christensenia-M. laxa* clade. This resolution was recovered across the parsimony analyses of varying *k*-values and the Bayesian analysis. Although *M. cicutifolia* and *E. kaulfussii* were sisters and together formed a sister clade to *M. vodrazkae* in the Bayesian analysis, in the parsimony analyses *M. vodrazkae* was constantly the sister of *E. kaulfussii* and these formed the sister clade of *M. cicutifolia*. These three terminals formed the sister group of *Ptisana* in all of the analyses. In the Bayesian analysis, the relationships of these two clades with *Danaea* and the remaining species of *Marattiopsis* remained unresolved. In the parsimony analyses, *Danaea* was constantly sister to *Marattiopsis* and the remaining extant Marattiaceae. Within *Marattiopsis*, *M. anglica* Thomas, *M. patagonica* Escapa et al. and *M. asiatica* Kawasaki formed a clade under the implied weights but remained unresolved under the equal weights. In the Bayesian analysis and in parsimony analyses with *k* = 5 and *k* = 10, the fossil genus *Danaeopsis* was resolved as the sister to the clade of the extant Marattiaceae and fossil *Marattiopsis*; these together formed a sister clade to the fossil genus *Qasimia*. With the value *k* = 15 (and *k* = 20) the relative positions of *Qasimia* and *Danaeopsis* were interchanged so that *Qasimia* was the sister of the most exclusive clade containing all the extant Marattiaceae. In all analyses, *Qasimia*, *Danaeopsis*, *Marattiopsis* and the extant Marattiaceae formed a clade that excluded all the remaining species in the analyses and are here considered as members of the family Marattiaceae.

The remaining species, that is Psaroniaceae, either remained largely unresolved (Bayesian and equally weighted parsimony) or had good but contradicting resolutions (implied weighted parsimony). However, *Sydneia manleyi* and *Radstockia kidstonii* Taylor were constantly resolved as sisters of each other, and they almost constantly formed the sister lineage to the remaining Marattiales (implied weighted parsimony) or were resolved outside the remaining Marattiales (Bayesian). Furthermore, *Danaeites rigida* Gu & Zhi and *Millaya tularosana* Mapes & Schabilion constantly formed a clade, either in an unresolved position (Bayes, equally weighted parsimony) or they were a sister of Marattiaceae (*k* = 5, *k* = 10), or sister of a large clade including Marattiaceae and the remaining Psaroniaceae (*k* = 15, *k* = 20). *Araiangium pygmaeum*

(Graham) Millay (*k* = 15, *k* = 20) and *Gemellitheca saudica* Wagner et al. (*k* = 5, *k* = 10) also were invariably resolved outside of the Psaroniaceae, but otherwise the family remained a monophyletic sister of Marattiaceae in the implied weighted parsimony analyses.

The parsimony dating of the total-evidence phylogeny resulted in an age estimate ranging from 307 Ma (BUR_{min}) to 320 Ma (BUR_{max}) for the Marattiales. The split between *Danaea* and the rest of the extant Marattiaceae was estimated to have occurred in the Late Triassic (201–236 Ma). *Angiopteris* was estimated to have separated during the Late Triassic–early Jurassic at the same time with the splitting of *Christensenia-M. laxa* and *Ptisana-Eupodium* clades. The estimated age range for the *Christensenia-M. laxa* split was extremely large due to the lack of any internal fossils and phylogenetic uncertainty in bootstrapping. However, the weighted mean age computed over the BS replicates placed this split at the late Jurassic. The split between *Ptisana* and *Eupodium* was placed at the Late Cretaceous. In this case, the fossil *Marattiopsis vodrazkae* provided an internal calibration point as sister of *E. kaulfussii*, but because the phylogenetic position of *Ptisana* was stable across the BS replicates, it was fixed in the time tree just below the *Eupodium*.

Biogeographical reconstructions

Our biogeographical reconstruction based on the DEC model and parsimony-dated phylogeny supports the North American origin of Marattiales during the Pennsylvanian (Fig. 4). The branches leading to Marattiaceae and the most recent common ancestor (MRCA) of the extant Marattiaceae were reconstructed as having a Eurasian origin. According to the reconstructed history, the genus *Danaea* reached its current South American distribution from the ancestral Eurasian range through North America while these continents were still connected. *Marattiopsis patagonica* was reconstructed to have spread via the same route independently. The *Ptisana-Eupodium* clade shows dispersal from the ancestral Eurasian range to Africa followed by expansion throughout the Gondwana that was still intact at that time, with a more recent split between the palaeotropical *Ptisana* and Antarctic-Neotropical *Eupodium* (including *M. vodrazkae*). The origin of the *Christensenia-M. laxa* clade was linked with dispersal from the ancestral Eurasian range to the directly connected Oceania, from where the *Marattia* was modelled to have reached its current Central American–Hawaiian range through Eurasia. *Angiopteris* originated within the ancestral Eurasian range, from where it was estimated to have reached its current range in Madagascar–India–Oceania–Australia
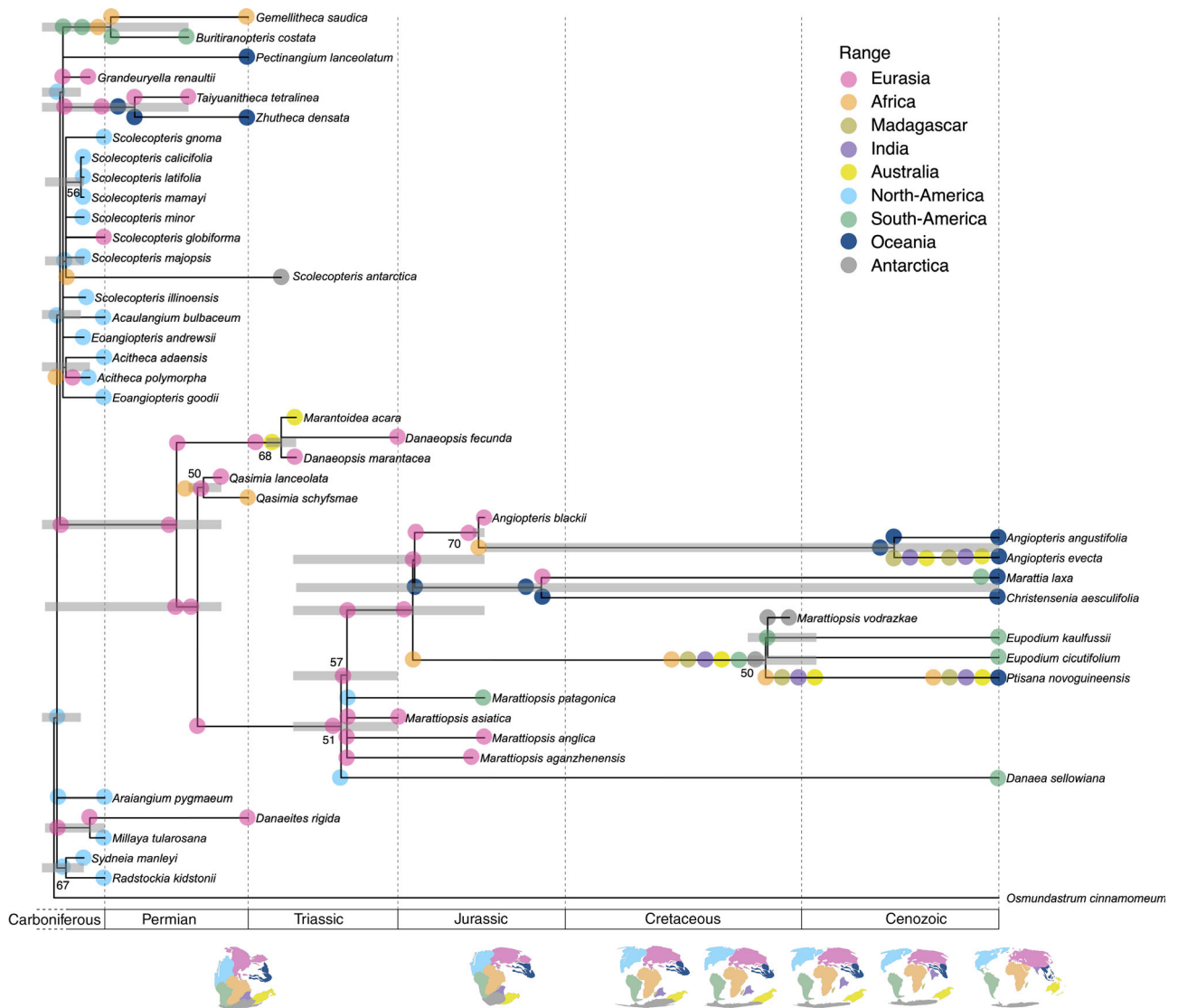
Fig. 4. Parsimony-dated phylogeny and Bayesian historical biogeography of the marattialean ferns. Grey bars represent the range of minimum age estimates (BUR_{min} to BUR_{max}) after excluding the youngest and oldest 2.5% of the age estimates, with the nodes positioned at the weighted average age calculated over the bootstrap replicates. The biogeographical scenario is based on DEC model using R/BIOGEOBEARS. The continental positions at the seven time intervals used in the biogeographical model are shown. Numbers indicate symmetrical resampling values >50%

by dispersal through Africa, where the genus is currently not present, to Oceania.

Within the fossil Psaroniaceae, several range expansions from the ancestral range in North America to Eurasia, South America, and Africa were inferred. These continents were connected at the time of these range expansions. The sole survivor of *Scolecopteris* Zenker into the Mesozoic, *S. antarctica* Delevoryas et al. (Delevoryas et al., 1992), was modelled to have dispersed from North America to Antarctica through Africa; all of these continents were connected during that time.

Discussion

Marattialean phylogenetics

Our results agree with the now widely supported view that Marattiales is the sister lineage of the leptosporangiate ferns (Knie et al., 2015; Lu et al., 2015; Rothfels et al., 2015; Qi et al., 2018; Lehtonen and Cárdenas, 2019). The persisting questions include the phylogenetic relationships between the extant genera—especially their rooting (Murdock, 2008b)—as well as how the extinct *Marattiopsis* is related to the extant

taxa (Escapa et al., 2014; Kvaček, 2014), and how the Palaeozoic forms are related to the morphologically modern forms (Mamay, 1950; Stidd, 1974; Hill et al., 1985).

Murdock (2008b) resolved the root of extant Marattiaceae on the branch connecting *Danaea* with the remaining genera but noted that the root position was sensitive to the dataset, outgroup choice and optimality criteria used. We also found the root on this branch in most analyses, but despite much larger datasets the alternative phylogenetic resolutions and root positions persisted depending on the data and optimality criterion applied. Murdock (2008b) noted that the branch leading to *Danaea* is the longest internal branch and therefore this rooting could represent a case of long-branch attraction (Bergsten, 2005). We recovered this root position in all of the analyses except the Bayesian analyses of plastome and total-evidence data. The same root position also was recovered in the ML analysis of 146 nuclear genes by Qi et al. (2018), who sampled four genera of Marattiaceae (*Marattia* and *Eupodium* were not sampled). Our total-evidence analyses also effectively broke down the long branch leading to *Danaea*, yet recovered the same root position under the parsimony analysis. However, in the Bayesian total-evidence tree the relationships between *Danaea*, *Ptisana-Eupodium* and *Angiopteris-Marattia-Christensenia* clades remain uncertain, and with extant taxa only, the root position is displaced from the *Danaea* branch. It has been noted that the Mk model may not be suitable for morphological datasets (Goloboff et al., 2019). However, as we recovered the root along the *Danaea* branch in the Bayesian analyses for phenotypic data (albeit with the topologies slightly different from the parsimony topologies), this may not be the problem in our case. Instead, it appears that the root position in the Bayesian analyses of plastome data depends on the outgroup; so that the analyses with *Osmundastrum* as the sole outgroup misplace the root as compared to the analysis incorporating a wider sampling of fern and seed plant plastomes.

Christensenia is a distinctive, and in many respects, highly autapomorphic genus (Hill and Camus, 1986a; Murdock, 2008b; Liu et al., 2019). This genus remained somewhat unstable in our analyses. Unlike Murdock (2008b) or Rothwell et al. (2018), we found that the most plausible phylogenetic position for *Christensenia* is a sister relationship with *Marattia*. An alternative position, supported by the plastome data under parsimony and phenotypic evidence, resolved *Christensenia* as a distinct lineage splitting off after *Danaea* had been separated from the rest of the Marattiaceae. Our analyses also recovered *Marattia cicutifolia*, a species previously not included in phylogenetic analyses, as more closely related to *E. kaulfussii* than *M. laxa* (*M. laxa* is the sister of *M. alata* Sw., the type of the

genus; Murdock, 2008a). Hence, we transfer *M. cicutifolia* into *Eupodium* (see Taxonomy below).

The systematic significance of the name *Marattiopsis* has recently been re-evaluated by palaeobotanists (Bomfleur et al., 2013; Escapa et al., 2014; Kvaček, 2014). After noting that several morphological features defining the genera now segregated from *Marattia* s.l. can be found mixed in the fossil taxa, they concluded that a broadly defined (i.e. paraphyletic) *Marattiopsis* is needed to accommodate the fragmentary fossil material (Bomfleur et al., 2013; Escapa et al., 2014; Kvaček, 2014). However, Escapa et al. (2014) considered most of the fossil species to probably be closest to *Ptisana*. We coded five *Marattiopsis* species for our analyses and found that *M. vodrazkae* from the Campanian of Antarctica was resolved in *Eupodium*, whereas the position of *M. aganzhenensis* (Yang et al.) Escapa et al. remained ambiguous and the remaining three species formed a clade in our preferred tree ($k = 15$, the same topology also was recovered under $k = 5$ and $k = 20$). It may therefore be possible to assign at least some fossils into the modern segregate genera, most notably *M. vodrazkea* and another unnamed but similarly stalked marattialean synangia from Antarctica (Vera and Césari, 2016) into *Eupodium*. It should be noted, however, that Rothwell et al. (2018) resolved these taxa differently.

The appearance of apparently modern Marattiaceae in the Mesozoic with distinctive morphologies compared to the Palaeozoic forms has puzzled palaeobotanists (Mamay, 1950; Stidd, 1974; Delevoryas et al., 1992; Zhifeng and Thomas, 1993). Our results suggest that the Permian *Qasimia* and Triassic *Danaeopsis*, two genera with taeniopteroid foliage, are among the oldest Marattiaceae. The sporangia of *Qasimia* are bilaterally fused into a synangia closely resembling some of the extant forms (Hill et al., 1985). However, in *Danaeopsis* the sporangia are arranged in two rows covering the entire lower lamina and are not fused into a synangia as in extant forms (Kustatscher et al., 2012). This topology is somewhat comparable with the results of Rothwell et al. (2018), who resolved these genera nested within the Marattiaceae. Apparently *Qasimia* never survived the Permian mass extinction, but *Danaeopsis* became an important component of the Triassic floras (Kustatscher et al., 2012). Some of our analyses ($k = 5$, $k = 20$, Bayesian) resolved these genera in reversed positions, which better fits the stratigraphy.

Considering Psaroniaceae, we found support for recognizing the subfamily Sydneideae extended to include not only *Sydneia* but also *Radstockia*, another genus with sphenopteroid foliage. We thus resolved this subfamily outside of the family, as sister to the remaining Marattiales. Rothwell et al. (2018) also found *Radstockia* as sister to the rest of Marattiales, although

their analysis placed *Sydneia* in a distant position deeply embedded in Psaroniaceae. The importance of *Radstockia* in understanding marattialean evolution has been recognized earlier and our finding may help to understand the origin and still unknown relationships of the marattialeans with other Palaeozoic ferns (Mamay, 1950; Stidd, 1974; Delevoryas et al., 1992). However, further resolution requires a taxonomically broader total-evidence analysis that also would include fossils related to Osmundales (Wang et al., 2014; Grimm et al., 2015) and other Palaeozoic ferns (Rothwell and Nixon, 2006). The close relationship between *Millaya* and *Danaeites* recognized here has been suggested before (Mapes and Schabilion, 1979b), but our preferred tree excludes them from the Psaroniaceae. Because the resolution within Psaroniaceae remained highly unstable, the relationships within this family are not discussed further. We note, however, that *Gemellitheca* Wagner et al. and *Buritiranopteris* Tavares et al. generally were resolved as early radiations and often as sisters, thus supporting similar resolutions for these taxa by Rothwell et al. (2018), and that we generally recovered monophyletic *Scolecopteris*.

Time-calibration and historical biogeography of Marattiales

Tip-dating phylogenies by coding fossil taxa as such into a total-evidence analyses has been considered as an alternative to the more widely used indirect dating approach of calibrating nodes with minimum age estimates taken from the fossil record (Ronquist et al., 2012a; Grimm et al., 2015). The inherent problem of the latter approach is the uncertainty in the phylogenetic placement of fossil calibration points (Ronquist et al., 2012a). Another problem is that multiple calibration priors may interact with each other and with other priors and thus influence the effective priors in an unpredictable way (Grimm et al., 2015). We included multiple calibration priors into our random local clock analysis of taxonomically broad plastome data to better model the presumed rate shifts. However, the result was that the effective priors in some cases strongly deviated from the specified priors and despite running a large number of long chains, the runs never properly converged. Our attempts to tip-date the marattialean tree using a Bayesian total-evidence approach likewise failed due to convergence issues. Hence, we relied on a model-free parsimony dating approach (Sterli et al., 2013) to infer the phylogenetic position of the fossil taxa and the uncertainty ranges for the node ages.

Although these methods are not commonly used in phylogenetic analyses of extant taxa, model-free calibration approaches have been applied before to datasets dominated by fossils (e.g. Laurin, 2004; Marjanović

and Laurin, 2007; Wang and Lloyd, 2016; Lloyd et al., 2016). In this latter case, where missing data are abundant, model assumptions regarding character change rates—and subsequent branch lengths—are not always fulfilled (Lloyd et al., 2016). Consequently, approaches assigning minimum node ages on the basis of stratigraphic data might be deemed as more conservative under those circumstances (Wang and Lloyd, 2016; Lloyd et al., 2016). However, it should be noted that these calibration methods are still prone to produce zero-length branches and subsequently misestimate divergence times when the fossil record is poorly sampled (Wang and Lloyd, 2016). To avoid this problem, authors have commonly employed a fixed minimum branch length (Marjanović and Laurin, 2007; Lloyd et al., 2016). Nevertheless, setting a minimum branch length is hardly straightforward because it is dependent on the taxonomic sampling, tree topology and the quality of the fossil record, hence arbitrarily fixed most of the time (Marjanović and Laurin, 2007; Sterli et al., 2013; Wang and Lloyd, 2016). In our analyses, the selection of a minimum branch length followed Sterli et al. (2013).

The parsimony dating resulted in a minimum age estimate of 201–236 Ma (Late Triassic) for the most recent common ancestor (MRCA) of the extant Marattiaceae. This closely corresponds with the Bayesian estimations of 185–224 Ma for this node by Lehtonen et al. (2017), who considered *Marattiopsis asiatica* as a member of *Ptisana* and hence constrained the origin of *Ptisana* at 176 Ma. They also estimated a similar age (214–242 Ma) for the origin of Marattiaceae directly from the fossil evidence (Lehtonen et al., 2017). Smith et al. (2010) also dated the MRCA of extant Marattiaceae at the Triassic–Jurassic boundary by using an internal calibration of *Marattia-Angiopteris* split at 166.1 Ma. By contrast, Testo and Sundue (2016) did not assign any calibration points inside Marattiaceae and they obtained a much younger estimate of 154–165 Ma for the MRCA of Marattiaceae. Even more dramatically different was our poorly converged BEAST estimate of just 76–06 Ma for this node (Fig. 2), also inferred without internal calibration points within Marattiaceae. Marattialean ferns are known to have an anomalously slow rate of molecular evolution (Soltis et al., 2002), perhaps reflecting their long generation time (Sharpe, 1993), as suggested previously for the tree ferns with a similarly slow rate of molecular evolution (Korall et al., 2010). Consequently, correctly modelling the evolutionary rate of Marattiales in the absence of close relatives may be extremely difficult and we consider our parsimony approach better justified in this case.

Our DEC model suggested a North American origin for Marattiales as a whole, as well as for Psaroniaceae, and a Eurasian origin for the Marattiaceae. According to this scenario, *Danaea* dispersed to its current

neotropical range through North America and *M. patagonica* independently dispersed the same route. *Danaea* fossils have been reported from North America, although they have been later considered misidentified (Collinson, 2001). The distribution of other extant genera likewise follow the patterns of continental breakup during the Mesozoic. The sister genera *Ptisana* and *Eupodium* are biogeographically disjunct; the former has a Palaeotropical range and the latter Neotropical. According to our model, this pattern is a result of dispersal from Eurasia through Africa to southern Pangaea, while all of these continents were still connected, and then splitting between the Neotropical-Antarctic *Eupodium* lineage and Palaeotropical *Ptisana*. In our tree (Fig. 4), this split is dated by the Campanian *Marattiopsis vodrazkae* (Kvaček, 2014). However, if the similarly stalked synangia from the Lower Cretaceous of Antarctica (Vera and Césari, 2016) also belong to *Eupodium*, the split between *Ptisana* and *Eupodium* would perfectly match the breakup of Africa from the Antarctica (Jokat et al., 2003). Murdock (2008b) briefly commented on the biogeography of *Marattia* by considering the following two alternative scenarios: the current distribution in the American tropics and Hawaii was achieved either by dispersal from the American continent to Hawaii, or vice versa. Our model suggests that the ancestor of the *Marattia-Christensenia* lineage dispersed from Eurasia to Southeast Asia and thus favours the Oriental origin of *Marattia*. Furthermore, our model suggests a Eurasian origin for *Angiopteris*. Thus, each of the extant main clades seem to have originated in different parts of the Pangaea as it was breaking up. This separation was probably promoted by palaeoclimatic patterns with *Marattia-Christensenia* restricted to far east, *Angiopteris* to Eurasia, *Danaea* to North America, and *Ptisana-Eupodium* to the Southern Hemisphere, where moist climates were available (see Escapa et al., 2014: fig. 8).

Plastome evolution

Comparative genome analysis across embryophytes has greatly improved our understanding about plastid genome evolution. The first plastid genome studies masked the divergent features of these molecules due to sampling biased towards angiosperms. Recent studies in ferns, however, have exposed dynamism that shape the molecular evolutionary landscape of this organelle (Labiak and Karol, 2017; Kuo et al., 2018; Robison et al., 2018; Lehtonen and Cárdenas, 2019). Fern plastomes show striking evidence of lineage specific re-arrangements shaped by multiple inversion and shifts in gene content depicting the dynamic nature of organellar genome evolution.

Our family-scale comparative genome analysis revealed previously unreported features of marattialean plastid genome evolution. The *mat*K gene is located within the *trn*K intron in all embryophytes except in non-Osmundales leptosporangiate ferns, where this gene has lost its flanking regions (Wolf et al., 2010). The presence of the *trn*K intron has previously been reported from Osmundales (Duffy et al., 2009) and from *Angiopteris evecta* (Roper et al., 2007). Our study confirms that the loss of *trn*K appeared in non-Osmundales leptosporangiate ferns by confirming the presence of *trn*K in all extant marattialean genera. Previous studies reported the pseudogenization of the highly divergent gene coding for the hypothetical protein *ycf*1 in *A. evecta* (Roper et al., 2007). This gene is interspersed by an 817-bp direct repeat, which is missing from the other marattialean fern plastid genomes. Thus, the pseudogenization of this gene seems to be autapomorphic in *A. evecta*, because *ycf*1 genes remain functional in other Marattiaceae. The divergence of this specific gene is not surprising because many other insertions and deletions have been reported from other embryophytes. For example, the degradation of this gene is almost exclusively accounted for by the plastome size reduction in the graminid clade of Poaceae (Poczai and Hyvönen, 2017).

The gene order in Marattiaceae showed high similarity to those observed in seed plants as members of the family showed only the *trn*G-*trn*T inversion characteristic to all ferns. The plastid genome structure evolution in Marattiaceae has remained constant, because the sequenced plastomes showed high synteny among all extant genera (Fig. 1). This could be correlated with evolutionary trends in the family implicating a correlation between slower genome structure and morphological evolution, also suggested by Roper et al. (2007). A recent study highlighted the importance of MORFFO-type mobile elements adjacent to inversion sites in shaping the plastid genome evolution of ferns (Robison et al., 2018). The origin and function of these elements are unknown, but they appear to be linked with the structural genome evolution. We identified and characterized these elements in Marattiaceae and found that MORFFO elements are absent from *Danaea*, *Marattia* and *Ptisana* but they are partially present in intergenic-spacer regions (IGS) of *Angiopteris*, *Christensenia* and *Eupodium*. The lack of relative abundance of such elements could partially explain the absence of dynamic genomic re-arrangements in Marattiaceae. However, the observed MORFFO2 and MORFFO3 elements in *Angiopteris* and *Christensenia* matched a single ORF (ORF531) in the plastome of *Mankyua* (Ophioglossales), suggesting that these elements may share a common origin in early diverging ferns, even if they are often found in distinct positions within the plastomes of the leptosporangiate ferns (Lehtonen and Cárdenas, 2019). Kim and Kim (2018) suggested that this ORF may be of

bacterial origin. We further matched the MORFFO1 element found in the two *Eupodium* species with the ORF295 in *Mankyua*. This ORF was found to be similar to the protein found in green alga (Kim and Kim, 2018). In *Eupodium* this ORF is associated with tandem repeats, and is located within a 1378-bp-long insertion. It was speculated that such plastome ORF insertions could originate from intercellular transfer from the mitochondrial genome (Logacheva et al., 2017). Some of these ORFs encode functional proteins, whereas others contain conserved domains or have become pseudogenes. Such structural changes in the plastome show greater complexity as compared to simple nucleotide substitutions (e.g. Poczai and Hyvönen, 2013), and such changes could be good phylogenetic markers.

Taxonomy

Eupodium cicutifolium (Kaulf.) Lehtonen, **comb.n.** ≡ *Marattia cicutifolia* Kaulf., Enum. Filic.: 32. 1824. – Syntypes: Brazil, *Martius s.n.* (syntype: M) and *Sellow s.n.* (syntype: B, destroyed?, PCR). For synonymy see Murdock (2017).

The genus *Eupodium* has been considered to contain two (Murdock, 2008a) or three (Christenhusz, 2010) species. The genus is diagnosed based on the presence of usually only a single leaf at a time, stalked synangia, and awns on the midrib of the pinnae. Murdock (2008b) did not sample *M. cicutifolia*, but nevertheless placed the species in *Marattia* s.s. because it has morphological characters more typical of that genus, despite of having shortly stalked synangia in some cases (Murdock, 2008a). Another morphological character common to *M. cicutifolia* and *Eupodium* is the spinulose exospore ornamentation (del Carmen Lavalle et al., 2011), which is quite similar to that found in *Angiopteris*, *Christensenia* and *Danaea* (Camus, 1990), but distinct from the granular to rugose ornamentation of spores in *Marattia* (del Carmen Lavalle et al., 2011) and *Ptisana* (Camus, 1990; Murdock, 2008a). The absence of awns, the presence of multiple leaves simultaneously, and general synangial and foliar characteristics in *M. cicutifolia* are more similar to *Marattia* and *Ptisana*. The phylogenetic position of *M. cicutifolia* in this study necessitates its transfer to *Eupodium*, but at the same time partly negates the morphological circumscription of the genus. Under the current circumscription, only the stalked synangia is diagnostic for *Eupodium*, but this character is not always clearly developed in *E. cicutifolium*. Biogeographically *Eupodium* remains a South American genus with a few occurrences in Central America and Hispaniola (Christenhusz, 2010), whereas *Marattia* is now restricted to Central America, Hawaii, Jamaica and Cuba (Murdock, 2008a).

References

Altschul, S.F., Gish, W., Miller, W., Myers, E.W. and Lipman, D.J., 1990. Basic local alignment search tool. J. Mol. Biol. 215, 403–410.

Amiryousefi, A., Hyvönen, J. and Poczai, P., 2018. The chloroplast genome sequence of bittersweet (*Solanum dulcamara*): plastid genome structure evolution in Solanaceae. PLoS ONE, 13, e0196069.

Arana, M.D., 2016. Familia Marattiaceae Kaulf. In: Anton, A.M. and Ponce, M.M. (Eds.), Flora Vascular de la República Argentina 2: Licofitas, Helechos, Gymnospermae. Instituto Multidisciplinario de Biología Vegetal, San Isidro, pp. 209–210.

Beier, S., Thiel, T., Münch, T., Scholz, U. and Mascher, M., 2017. MISA-web: a web server for microsatellite prediction. Bioinformatics 33, 2583–2585.

Bergsten, J., 2005. A review of long-branch attraction. Cladistics 21, 163–193.

Bomfleur, B., Escapa, I.H., Taylor, E.L. and Taylor, T.N., 2013. (2151) Proposal to conserve the name *Marattiopsis* (fossil Marattiaceae) with a conserved type. Taxon 62, 637–638.

Bomfleur, B., McLoughlin, S. and Vajda, V., 2014. Fossilized nuclei and chromosomes reveal 180 million years of genomic stasis in royal ferns. Science 343, 1376–1377.

Bomfleur, B., Grimm, G.W. and McLoughlin, S., 2017. The fossil Osmundales (Royal Ferns)—a phylogenetic network analysis, revised taxonomy, and evolutionary classification of anatomically preserved trunks and rhizomes. PeerJ 5, e3433.

Camus, J.M., 1990. Marattiaceae. In: Kubitzki, K. (Ed.), The Families and Genera of Vascular Plants. v. 1: Pteridophytes and Gymnosperms. Springer, Berlin, pp. 174–180.

Capella-Gutierrez, S., Silla-Martinez, J.M. and Gabaldon, T., 2009. trimAl: a tool for automated alignment trimming in large-scale phylogenetic analyses. Bioinformatics 25, 1972–1973.

del Carmen Lavalle, M., 2003. Taxonomía de las especies neotropicales de *Marattia* (Marattiaceae). Darwiniana. 41, 61–86.

del Carmen Lavalle, M., 2007. Caracteres diagnósticos foliares en especies neotropicales de *Marattia* Sw. (Marattiaceae-Pteridophyta). Ann. Missouri Bot. Gard. 94, 192–201.

del Carmen Lavalle, M., Mengascini, A. and Rodríguez, M., 2011. Morfología de esporas y sinangios en especies neotropicales del helecho *Marattia* (Marattiaceae). Rev. Biol. Trop. 59, 1833–1844.

Carter, A., Riley, T.R., Hillenbrand, C.-D. and Rittner, M., 2017. Widespread Antarctic glaciation during the Late Eocene. Earth Planet. Sci. Lett. 458, 49–57.

Christenhusz, M.J.M., 2007. Evolutionary history and taxonomy of Neotropical marattioid ferns: studies of an ancient lineage of plants. Ann. Univ. Turku. ser. AII. 216, 1–78.

Christenhusz, M.J.M., 2010. Revision of the Neotropical fern genus *Eupodium* (Marattiaceae). Kew Bull. 65, 115–121.

Christenhusz, M.J.M. and Chase, M.W., 2014. Trends and concepts in fern classification. Ann. Bot. 113, 571–594.

Christenhusz, M.J.M., Tuomisto, H., Metzgar, J.S. and Pryer, K.M., 2008. Evolutionary relationships within the Neotropical, eusporangiate fern genus *Danaea* (Marattiaceae). Mol. Phylogenet. Evol. 46, 34–48.

Cleal, C.J., 2015. The generic taxonomy of Pennsylvanian age marattialean fern frond adpressions. Palaeontogr. Abt. B. 292, 1–21.

Collinson, M.E., 2001. Cainozoic ferns and their distribution. Brittonia 53, 173–235.

Crisp, M.D., Hardy, N.B. and Cook, L.G., 2014. Clock model makes a large difference to age estimates of long-stemmed clades with no internal calibration: a test using Australian grasstrees. BMC Evol. Biol. 14, 263.

Der, J.P., 2010. Genomic perspectives on evolution in bracken fern. Doctoral thesis, Utah State University.

Delevoryas, T., Taylor, T.N. and Taylor, E.L., 1992. A marattialean fern from the Triassic of Antarctica. Rev. Palaeobot. Palynol. 74, 101–107.

Dierckxsens, N., Mardulyn, P. and Smits, G., 2016. NOVOPlasty: de novo assembly of organelle genomes from whole genome data. Nucleic Acids Res., 45, e18.

DiMichele, W.A. and Phillips, T.L., 2002. The ecology of Paleozoic ferns. Rev. Palaeobot. Palynol. 119, 143–159.

Drummond, A.J. and Suchard, M.A., 2010. Bayesian random local clocks, or one rate to rule them all. BMC Biol. 8, 114.

Duffy, A.M., Kelchner, S.A. and Wolf, P.G., 2009. Conservation of selection on *mat*K following an ancient loss of its flanking intron. Gene 438, 17–25.

Escapa, I.H., Bomfleur, B., Cúneo, N.R. and Scasso, R., 2014. A new marattiaceous fern from the Lower Jurassic of Patagonia (Argentina): the renaissance of *Marattiopsis*. J. Syst. Palaeontol. 13, 677–689.

Falcon-Lang, H.J., 2005. Small cordaitalean trees in a marine-influenced coastal habitat in the Pennsylvanian Joggins Formation, Nova Scotia. J. Geol. Soc. 162, 485–500.

Fitzhugh, K., 2006. The "requirement of total evidence" and its role in phylogenetic systematics. Biol. Philos. 21, 309–351.

Gao, L., Yi, X., Yang, Y.X., Su, Y.J. and Wang, T., 2009. Complete chloroplast genome sequence of a tree fern *Alsophila spinulosa*: insights into evolutionary changes in fern chloroplast genomes. BMC Evol. Biol. 9, 130.

Gao, L., Zhou, Y., Wang, Z.-W., Su, Y.-J. and Wang, T., 2011. Evolution of the *rpoB-psbZ* region in fern plastid genomes: notable structural rearrangements and highly variable intergenic spacers. BMC Plant Biol. 11, 64.

Gao, L., Wang, B., Wang, Z.-W., Zhou, Y., Su, Y.-J. and Wang, T., 2013. Plastome sequences of *Lygodium japonicum* and *Marsilea crenata* reveal the genome organization transformation from basal ferns to core leptosporangiates. Genome Biol. Evol. 5, 1403–1407.

Gernhard, T., 2008. The conditioned reconstructed process. J. Theor. Biol. 253, 769–778.

Gerrienne, P., Fairon-Demaret, M. and Galtier, J., 1999. A Namurian A (Silesian) permineralized flora from the Carrière du Lion at Engihoul (Belgium). Rev. Palaeobot. Palynol. 107, 1–15.

Gitzendanner, M.A., Soltis, P.S., Wong, G.K.S., Ruhfel, B.R. and Soltis, D.E., 2018. Plastid phylogenomic analysis of green plants: a billion years of evolutionary history. Am. J. Bot. 105, 291–301.

Goloboff, P.A., 1999. Analyzing large data sets in reasonable times: solutions for composite optima. Cladistics 15, 415–428.

Goloboff, P., 2003. Improvements to resampling measures of group support. Cladistics 19, 324–332.

Goloboff, P.A., 2014. Extended implied weighting. Cladistics 30, 260–272.

Goloboff, P.A. and Catalano, S.A., 2016. TNT version 1.5, including a full implementation of phylogenetic morphometrics. Cladistics 32, 221–238.

Goloboff, P.A., Pittman, M., Pol, D. and Xu, X., 2019. Morphological data sets fit a common mechanism much more poorly than DNA sequences and call into question the Mkv model. Syst. Biol. 68, 494–504.

Grewe, F., Guo, W., Gubbels, E.A., Hansen, A.K. and Mower, J.P., 2013. Complete plastid genomes from *Ophioglossum californicum*, *Psilotum nudum*, and *Equisetum hyemale* reveal an ancestral land plant genome structure and resolve the position of Equisetales among monilophytes. BMC Evol. Biol. 13, 8.

Grimm, G.W., Kapli, P., Bomfleur, B., McLoughlin, S. and Renner, S.S., 2015. Using more than the oldest fossils: dating Osmundaceae with three Bayesian clock approaches. Syst. Biol. 64, 396–405.

Guindon, S., Dufayard, J.-F., Lefort, V., Anisimova, M., Hordijk, W. and Gascuel, O., 2010. New algorithms and methods to estimate maximum-likelihood phylogenies: assessing the performance of PhyML 3.0. Syst. Biol. 59, 307–321.

Guo, W., Grewe, F. and Mower, J.P., 2015. Variable frequency of plastid RNA editing among ferns and repeated loss of uridine-to-cytidine editing from vascular plants. PLoS ONE, 10, e0117075.

Guo, W., Zhu, A., Fan, W. and Mower, J.P., 2016. Complete mitochondrial genomes from the ferns *Ophioglossum californicum* and *Psilotum nudum* are highly repetitive with the largest organellar introns. New Phytol. 213, 391–403.

Han, J., Wang, M., Qiu, Q. and Guo, R., 2017. Characterization of the complete chloroplast genome of *Cycas panzhihuaensis*. Conserv. Genet. Resour. 9, 21–23.

Hao, S. and Xue, J., 2013. Earliest record of megaphylls and leafy structures, and their initial diversification. Chinese Sci. Bull. 58, 2784–2793.

Harris, T.M., 1961. The Yorkshire Jurassic Flora, 1. Thallophyta – Pteridophyta. British Museum of Natural History, London.

Harris, R.S., 2007. Improved pairwise alignment of genomic DNA. Ph.D. Thesis, The Pennsylvania State University.

He, X.-Z., Wang, S.-J. and Wang, J., 2016. *Chansitheca wudaensis* (Gleicheniaceae, fern) from the early Permian Wuda Tuff Flora, Inner Mongolia. Palaeoworld 25, 199–211.

Heled, J. and Drummond, A.J., 2011. Calibrated tree priors for relaxed phylogenetics and divergence time estimation. Syst. Biol. 61, 138–149.

Hill, C.R., 1987. Jurassic *Angiopteris* (Marattiales) from north Yorkshire. Rev. Palaeobot. Palynol. 51, 65–93.

Hill, C.R. and Camus, J.M. (1986a) Evolutionary cladistics of marattialean ferns. Bull. Br. Mus. Nat. Hist. 14, 219–300.

Hill, C.R. and Camus, J.M. (1986b) Pattern cladistics or evolutionary cladistics? Cladistics 2, 362–375.

Hill, C.R., Wagner, R.H. and El-Khayal, A.A., 1985. *Qasimia* gen. nov., an early *Marattia*-like fern from the Permian of Saudi Arabia. Scr. Geol. 79, 1–50.

Hoang, D.T., Chernomor, O., von Haeseler, A., Minh, B.Q. and Vinh, L.S., 2018. UFBoot2: improving the ultrafast bootstrap approximation. Mol. Biol. Evol. 35, 518–522.

Hu, S., Taylor, D.W., Brenner, G.J. and Basha, S.H., 2008. A new marsilealean fern species from the Early Cretaceous of Jordan. Palaeoworld. 17, 235–245.

Jin, J.-J., Yu, W.-B., Yang, J.-B., Song, Y., Yi, T.-S. and Li, D.-Z., 2018. GetOrganelle: a simple and fast pipeline for de novo assembly of a complete circular chloroplast genome using genome skimming data. bioRxiv 1–11.

Jokat, W., Boebel, T., König, M. and Meyer, U., 2003. Timing and geometry of early Gondwana breakup. J. Geophys. Res. 108, 91–15.

Jud, N.A., Rothwell, G.W. and Stockey, R.A., 2008. *Todea* from the Lower Cretaceous of western North America: implications for the phylogeny, systematics, and evolution of modern Osmundaceae. Am. J. Bot. 95, 330–339.

Kalyaanamoorthy, S., Minh, B.Q., Wong, T.K.F., von Haeseler, A. and Jermiin, L.S., 2017. ModelFinder: fast model selection for accurate phylogenetic estimates. Nat. Methods. 14, 587–589.

Karol, K.G., Arumuganathan, K., Boore, J.L., Duffy, A.M., Everett, K.D., Hall, J.D., Hansen, S.K., Kuehl, J.V., Mandoli, D.F., Mishler, B.D., Olmstead, R.G., Renzaglia, K.S. and Wolf, P.G., 2010. Complete plastome sequences of *Equisetum arvense* and *Isoetes flaccida*: implications for phylogeny and plastid genome evolution of early land plant lineages. BMC Evol. Biol. 10, 321.

Kim, H.T. and Kim, K.-J., 2018. Evolution of six novel ORFs in the plastome of *Mankyua chejuense* and phylogeny of eusporangiate ferns. Sci. Rep. 8, 16466.

Kim, H.T., Chung, M.G. and Kim, K.-J., 2014. Chloroplast genome evolution in early diverged leptosporangiate ferns. Mol. Cells. 37, 372–382.

Knie, N., Fischer, S., Grewe, F., Polsakiewicz, M. and Knoop, V., 2015. Horsetails are the sister group to all other monilophytes

and Marattiales are sister to leptosporangiate ferns. Mol. Phylogenet. Evol. 90, 140–149.

van Konijnenburg-van Cittert, J.H.A., 1975. Some notes on *Marattia anglica* from the Jurassic of Yorkshire. Rev. Palaeobot. Palynol. 20, 205–214.

Korall, P., Schuettpelz, E. and Pryer, K.M., 2010. Abrupt deceleration of molecular evolution linked to the origin of arborescence in ferns. Evolution 64, 2786–2792.

Krassilov, V. and Bacchia, F., 2000. Cenomanian florule of Nammoura, Lebanon. Cretac. Res. 21, 785–799.

Krzywinski, M., Schein, J., Birol, I., Connors, J., Gascoyne, R., Horsman, D., Jones, S.J. and Marra, M.A., 2009. Circos: an information aesthetic for comparative genomics. Genome Res. 19, 1639–1645.

Kuo, L.-Y., Qi, X., Ma, H. and Li, F.-W., 2018. Order-level fern plastome phylogenomics: new insights from Hymenophyllales. Am. J. Bot. 105, 1545–1555.

Kurtz, S., Phillippy, A., Delcher, A.L., Smoot, M., Shumway, M., Antonescu, C. and Salzberg, S.L., 2004. Versatile and open software for comparing large genomes. Genome Biol., 5, R12.

Kustatscher, E., Kelber, K.-P. and van Konijnenburg-van Cittert, J.H.A., 2012. *Danaeopsis* Heer ex Schimper 1869 and its European Triassic species. Rev. Palaeobot. Palynol. 183, 32–49.

Kvaček, J., 2014. *Marattiopsis vodrazkae* sp. nov. (Marattiaceae) from the Campanian of the Hidden Lake Formation, James Ross Island, Antarctica. Acta Mus. Nat. Pragae, Ser. B, Hist. Nat. 70, 211–218.

Labiak, P.H. and Karol, K.G., 2017. Plastome sequences of an ancient fern lineage reveal remarkable changes in gene content and architecture. Am. J. Bot. 104, 1008–1018.

Lanfear, R., Calcott, B., Ho, S.Y.W. and Guindon, S., 2012. PartitionFinder: combined selection of partitioning schemes and substitution models for phylogenetic analyses. Mol. Biol. Evol. 29, 1695–1701.

Lanfear, R., Frandsen, P.B., Wright, A.M., Senfeld, T. and Calcott, B., 2017. Partitionfinder 2: New methods for selecting partitioned models of evolution for molecular and morphological phylogenetic analyses. Mol. Biol. Evol. 34, 772–773.

Laurin, M., 2004. The evolution of body size, Cope's rule and the origin of amniotes. Syst. Biol. 53, 594–622.

Lehtonen, S., 2011. Towards resolving the complete fern tree of life. PLoS ONE, 6, e24851.

Lehtonen, S. and Cárdenas, G.G., 2019. Dynamism in plastome structure observed across the phylogenetic tree of ferns. Bot. J. Linn. Soc. 190, 229–241.

Lehtonen, S., Silvestro, D., Karger, D.N., Scotese, C., Tuomisto, H., Kessler, M., Peña, C., Wahlberg, N. and Antonelli, A., 2017. Environmentally driven extinction and opportunistic origination explain fern diversification patterns. Sci. Rep. 7, 4831.

Lesnikowska, A.D., 1989. Anatomically Preserved Marattiales from Coal Swamps of the Desmoinesian and Missourian of the Midcontinent United States: Systematics, Ecology and Evolution. University of Illinois, Urbana-Champaign, Illinois, USA.

Lesnikowska, A. and Galtier, J., 1991. A reconsideration of four genera of permineralized Marattiales from the Stephanian and Autunian of France. Rev. Palaeobot. Palynol. 67, 141–152.

Lesnikowska, A. and Galtier, J., 1992. Permineralized Marattiales from the Stephanian and Autunian of central France: a reinvestigation of *Grandeuryella renaultii* (Stur) Weiss emend. Rev. Palaeobot. Palynol. 72, 299–315.

Lewis, P.O., 2001. A likelihood approach to estimating phylogeny from discrete morphological character data. Syst. Biol. 50, 913–925.

Li, C.X. and Lu, S.G., 2007. Phylogeny and divergence of Chinese Angiopteridaceae based on chloroplast DNA sequence data (*rbcL* and *trnL-F*). Chinese Sci. Bull. 52, 91–97.

Li, F.-W., Kuo, L.-Y., Pryer, K.M. and Rothfels, C.J., 2016. Genes translocated into the plastid inverted repeat show decelerated substitution rates and elevated GC content. Genome Biology and Evolution 8, 2452–2458.

Li, F.-W., Brouwer, P., Carretero-Paulet, L., Cheng, S., Vries, J., Delaux, P.-M., Eily, A., Koppers, N., Kuo, L.-Y., Li, Z., *et al.*,

2018. Fern genomes elucidate land plant evolution and cyanobacterial symbioses. Nature Plants. 4, 460–472.

Li, H., Handsaker, B., Wysoker, A., Fennell, T., Ruan, J., Homer, N., Marth, G., Abecasis, G., Durbin, R. and 1000 Genome Project Data Processing Subgroup, 2009. The sequence alignment/map format and SAMtools. Bioinformatics 25, 2078–2079.

Liu, H., Schneider, H., Yu, Y., Fuijwara, T. and Khine, P.K., 2019. Towards the conservation of the Mesozoic relict fern *Christensenia*: a fern species with extremely small populations in China. J. Plant Res. 132, 601–616.

Liu, Z.H., Hilton, J. and Li, C.S. (2000a) Review on the origin, evolution and phylogeny of Marattiales. Chinese Bull. Bot. 17, 39–52.

Liu, Z.H., Li, C.S. and Hilton, J. (2000b) *Zhutheca* Liu, Li et Hilton gen. nov., the fertile pinnules of *Fascipteris densata* Gu et Zhi and their significance in marattialean evolution. Rev. Palaeobot. Palynol. 109, 149–160.

Liu, Z.H., Li, C-s and Hilton, J., 2001. Fertile pinnules of *Danaeites rigida* Gu and Zhi (Marattiales) from the Upper Permian of south China. Bot. J. Linn. Soc. 136, 107–117.

Lloyd, G.T., Bapst, D.W., Friedman, M. and Davis, K.E., 2016. Probabilistic divergence time estimation without branch lengths: dating the origins of dinosaurs, avian flight and crown birds. Biol. Let. 12, 20160609.

Logacheva, M.D., Krinitsina, A.A., Belenikin, M.S., Khafizov, K., Konorov, E.A., Kuptsov, S.V. and Speranskaya, A.S., 2017. Comparative analysis of inverted repeats of polypod fern (Polypodiales) plastomes reveals two hypervariable regions. BMC Plant Biol. 17(Suppl 2), 255.

Lu, J.-M., Zhang, N., Du, X.-Y., Wen, J. and Li, D.-Z., 2015. Chloroplast phylogenomics resolves key relationships in ferns. J. Syst. Evol. 53, 448–457.

Mamay, S.H., 1950. Some American Carboniferous fern fructifications. Ann. Missouri Bot. Gard. 37, 409–476.

Mapes, G. and Schabilion, J. (1979a) A new species of *Acitheca* (Marattiales) from the Middle Pennsylvanian of Oklahoma. J. Paleontol. 53, 685–694.

Mapes, G. and Schabilion, J.T. (1979b) *Millaya* gen. n., an upper Paleozoic genus of marattialean synangia. Am. J. Bot. 66, 1164–1172.

Marjanović, D. and Laurin, M., 2007. Fossils, molecules, divergence times, and the origin of lissamphibians. Syst. Biol. 56, 369–388.

Matasci, N., Hung, L.-H., Yan, Z., Carpenter, E.J., Wickett, N.J., Mirarab, S., Nguyen, N., Warnow, T., Ayyampalayam, S., Barker, M. *et al.*, 2014. Data access for the 1,000 Plants (1KP) project. GigaScience. 3, 17.

Matzke, N.J. (2013a) Probabilistic historical biogeography: new models for founder-event speciation, imperfect detection, and fossils allow improved accuracy and model-testing. Front. Biogeogr., 5, 242–248.

Matzke, N.J., 2013b. BioGeoBEARS: Biogeography with Bayesian (and likelihood) evolutionary analysis in R scripts. R package, version 0.21. https://phylo.wikidot.com/biogeobears

Millay, M.A., 1977. *Acaulangium* gen. n. a fertile marattialean from the Upper Pennsylvanian of Illinois. Am. J. Bot. 64, 223–229.

Millay, M.A., 1978. Studies of Paleozoic marattialeans: the morphology and phylogenetic position of *Eoangiopteris goodii* sp. n. Am. J. Bot. 65, 577–583.

Millay, M.A., 1979. Studies of Paleozoic marattialeans: a monograph of the American species of *Scolecopteris*. Palaeontogr. Abt. B. 169, 1–69.

Millay, M.A., 1982. Studies of paleozoic marattialeans - the morphology and probable affinities of *Telangium pygmaeum* Graham. Am. J. Bot. 69, 1566–1572.

Millay, M.A., 1997. A review of permineralized Euramerican Carboniferous tree ferns. Rev. Palaeobot. Palynol. 95, 191–209.

Millay, M.A. and Galtier, J., 1990. Studies of Paleozoic marattialean ferns: *Scolecopteris globiforma* n.sp., from the Stephanian of France. Rev. Palaeobot. Palynol. 63, 163–171.

Miller, C.N.J., 1971. Evolution of the fern family Osmundaceae based on anatomical studies. Contr. Mus. Paleontol. Univ. Michigan. 23, 105–169.

Miller, M.A., Pfeiffer, W. and Schwartz, T., 2010. Creating the CIPRES science gateway for inference of large phylogenetic trees. In: Gateway Computing Environments Workshop GCE, pp. 1–8.

Morgan, E.J., 1959. The morphology and anatomy of American species of the genus *Psaronius*. III. Biol. Monogr. 27, 1–108.

Murdock, A.G. (2008a) A taxonomic revision of the eusporangiate fern family Marattiaceae, with description of a new genus *Ptisana*. Taxon 57, 737–755.

Murdock, A.G. (2008b) Phylogeny of marattioid ferns (Marattiaceae): inferring a root in the absence of a closely related outgroup. Am. J. Bot. 95, 626–641.

Murdock, A.G., 2017. Correcting confusion in Brazilian *Marattia* types. Taxon 66, 967–969.

Nazir, S. and Khan, M.S., 2012. Chloroplast-encoded *chl*B gene from *Pinus thunbergii* promotes root and early chlorophyll pigment development in *Nicotiana tabaccum*. Mol. Biol. Rep. 39, 10637–10646.

Nguyen, L.-T., Schmidt, H.A., von Haeseler, A. and Minh, B.Q., 2015. IQ-TREE: a fast and effective stochastic algorithm for estimating maximum-likelihood phylogenies. Mol. Biol. Evol. 32, 268–274.

One Thousand Plant Transcriptomes Initiative, 2019. One thousand plant transcriptomes and the phylogenomics of green plants. Nature 574, 679–685.

Phillips, T.L., Peppers, R.A. and DiMichele, W.A., 1985. Stratigraphic and interregional changes in Pennsylvanian coal-swamp vegetation - environmental inferences. Int. J. Coal Geol. 5, 43–109.

Phipps, C.J., Taylor, T.N., Taylor, E.L., Cúneo, N.R., Boucher, L.D. and Yao, X., 1998. *Osmunda* (Osmundaceae) from the Triassic of Antarctica: an example of evolutionary stasis. Am. J. Bot. 85, 888–895.

Poczai, P. and Hyvönen, J., 2013. Discovery of novel plastid phenylalanine (*trnF*) pseudogenes defines a distinctive clade in Solanaceae. Springerplus. 2, 459.

Poczai, P. and Hyvönen, J., 2017. The complete chloroplast genome sequence of the CAM epiphyte Spanish moss (*Tillandsia usneoides*, Bromeliaceae) and its comparative analysis. PLoS ONE, 12, e0187199.

Pol, D. and Norell, M.A., 2001. Comments on the Manhattan stratigraphic measure. Cladistics 17, 285–289.

Pol, D., Norell, M.A. and Siddall, M.E., 2004. Measures of stratigraphic fit to phylogeny and their sensitivity to tree size, tree shape, and scale. Cladistics 20, 64–75.

PPG I, 2016. A community-derived classification for extant lycophytes and ferns. J. Syst. Evol. 54, 563–603.

Pryer, K.M., Smith, A.R. and Skog, J.E., 1995. Phylogenetic relationships of extant ferns based on evidence from morphology and *rbcL* sequences. Am. Fern J. 85, 205–282.

Pryer, K.M., Schneider, H., Smith, A.R., Cranfill, R. and Wolf, P.G., 2001. Horsetails and ferns are a monophyletic group and the closest living relatives to seed plants. Nature 409, 618–622.

Pšenička, J., Bek, J., Zodrow, E.L., Cleal, C.J. and Hemsley, A.R., 2003. A new late Westphalian fossil marattialean fern from Nova Scotia. Bot. J. Linn. Soc. 142, 199–212.

Pšenička, J., Zodrow, E.L. and D'Angelo, J.A., 2014. Sterile foliage of fertile *Sydneia manleyi* and synangial chemistry (eusporangiate fern, Late Asturian, Canada): a new subfamily Sydneideae. Folia Mus. Rerum Nat. Bohemiae Occid. Geol. et Paleobiol. 47, 1–13.

Pyron, R.A., 2011. Divergence time estimation using fossils as terminal taxa and the origins of Lissamphibia. Syst. Biol. 60, 466–481.

Qi, X., Kuo, L.-Y., Guo, C., Li, H., Li, Z., Qi, J., Wang, L., Hu, Y., Xiang, J., Zhang, C. et al., 2018. A well-resolved fern nuclear phylogeny reveals the evolution history of numerous transcription factor families. Mol. Phylogenet. Evol. 127, 961–977.

Quinlan, A.R. and Hall, I.M., 2010. BEDTools: a flexible suite of utilities for comparing genomic features. Bioinformatics 26, 841–842.

Rambaut, A., 2006–2018. FigTree, version 1.4.4. http://tree.bio.ed.ac.uk/software/figtree/.

Rambaut, A. and Drummond, A.J., 2002–2018a. LogCombiner v1.10.1. https://beast.community/logcombiner.

Rambaut, A. and Drummond, A.J., 2002–2018b. TreeAnnotator v1.10.1. https://beast.community/treeannotator.

Rambaut, A., Drummond, A.J., Xie, D., Baele, G. and Suchard, M.A., 2018. Posterior summarization in Bayesian phylogenetics using Tracer 1.7. Syst. Biol. 67, 901–904.

Ranwez, V., Harispe, S., Delsuc, F. and Douzery, E.J.P., 2011. MACSE: multiple alignment of coding sequences accounting for frameshifts and stop codons. PLoS ONE, 6, e22594.

Ree, R.H. and Smith, S.A., 2008. Maximum likelihood inference of geographic range evolution by dispersal, local extinction, and cladogenesis. Syst. Biol. 57, 4–14.

Robison, T.A., Grusz, A.L., Wolf, P.G., Mower, J.P., Fauskee, B.D., Sosa, K. and Schuettpelz, E., 2018. Mobile elements shape plastome evolution in ferns. Genome Biol. Evol. 10, 2558–2571.

Rolleri, C., 1993. Revision of the genus *Christensenia*. Am. Fern J. 83, 3–19.

Rolleri, C.H., 2002. Caracteres diagnósticos y taxonomía en el género *Angiopteris* Hoffm. (Marattiaceae Bercht. & J. S. Presl): I, los caracteres. Rev. Mus. La Plata. 15, 23–49.

Rolleri, C., Lavalle, M.C., Mengascini, A. and Rodríguez, M., 1996. Spore morphology and systematics of the genus *Christensenia*. Am. Fern J. 86, 80–88.

Ronquist, F., Klopfstein, S., Vilhelmsen, L., Schulmeister, S., Murray, D.L. and Rasnitsyn, A.P. (2012a) A total-evidence approach to dating with fossils, applied to the early radiation of the Hymenoptera. Syst. Biol. 61, 973–999.

Ronquist, F., Teslenko, M., van der Mark, P., Ayres, D.L., Darling, A., Hohna, S., Larget, B., Liu, L., Suchard, M.A. and Huelsenbeck, J.P. (2012b) MrBayes 3.2: Efficient Bayesian phylogenetic inference and model choice across a large model space. Syst. Biol. 61, 539–542.

Roper, J.M., Hansen, S.K., Wolf, P.G., Karol, K.G., Mandoli, D.F., Everett, K.D.E., Kuehl, J. and Boore, J.L., 2007. The complete plastid genome sequence of *Angiopteris evecta* (G. Forst.) Hoffm. (Marattiaceae). Am. Fern J. 97, 95–106.

Rosenstock, E., 1912. Filices novo-guineenses Bamlerianae et Keysserianae. Repert. Spec. Nov. Regni Veg. 10, 321–343.

Rößler, R. and Galtier, J., 2002. First *Grammatopteris* tree ferns from the Southern Hemisphere - new insights in the evolution of the Osmundaceae from the Permian of Brazil. Rev. Palaeobot. Palynol. 121, 205–230.

Rothfels, C.J. and Schuettpelz, E., 2013. Accelerated rate of molecular evolution for vittarioid ferns is strong and not driven by selection. Syst. Biol. 63, 31–54.

Rothfels, C.J., Li, F.W., Sigel, E.M., Huiet, L., Larsson, A., Burge, D.O., Ruhsam, M., Deyholos, M., Soltis, D.E., Stewart, C.N. et al., 2015. The evolutionary history of ferns inferred from 25 low-copy nuclear genes. Am. J. Bot. 102, 1089–1107.

Rothwell, G.W., 1999. Fossils and ferns in the resolution of land plant phylogeny. Bot. Rev. 65, 188–209.

Rothwell, G.W. and Nixon, K.C., 2006. How does the inclusion of fossil data change our conclusions about the phylogenetic history of euphyllophytes? Int. J. Plant Sci. 167, 737–749.

Rothwell, G.W., Millay, M.A. and Stockey, R.A., 2018. Resolving the overall pattern of marattialean fern phylogeny. Am. J. Bot. 105, 1304–1314.

Sablok, G., Amiryousefi, A., He, X., Hyvönen, J. and Poczai, P., 2019. Sequencing the plastid genome of giant ragweed (*Ambrosia trifida*, Asteraceae) from a herbarium specimen. Front. Plant Sci. 10, 218.

Sarver, B.A.J., Pennell, M.W., Brown, J.W., Keeble, S., Hardwick, K.M., Sullivan, J. and Harmon, L.J., 2019. The choice of tree prior and molecular clock does not substantially affect phylogenetic inferences of diversification rates. PeerJ., 7, e6334.

Schimper, W.P., 1869. Traité de paléontologie végétale, ou, La flore du monde primitif dans ses rapports avec les formations géologiques et la flore du monde actuel. J. B. Baillière et Fils, Paris.

Schneider, H., Smith, A.R. and Pryer, K.M., 2009. Is morphology really at odds with molecules in estimating fern phylogeny? Syst. Bot. 34, 455–475.

Schneider, H., Liu, H., Clark, J., Hidalgo, O., Pellicer, J., Zhang, S., Kelly, L.J., Fay, M.F. and Leitch, I.J., 2015. Are the genomes of royal ferns

really frozen in time? Evidence for coinciding genome stability and limited evolvability in the royal ferns. New Phytol. 207, 10–13.

Schuettpelz, E. and Pryer, K.M., 2007. Fern phylogeny inferred from 400 leptosporangiate species and three plastid genes. Taxon 56, 1037–1050.

Scotese, C., 2016. PALEOMAP PaleoAtlas for GPlates and the PaleoData Plotter Program. PALEOMAP Project, http://www.earthbyte.org/paleomap-paleoatlas-for-gplates.

Senterre, B., Rouhan, G., Fabre, I., Morel, C. and Christenhusz, M.J.M., 2014. Revision of the fern family Marattiaceae in the Seychelles with two new species and a discussion of the African *Ptisana fraxinea* complex. Phytotaxa. 158, 57–19.

Serbet, R. and Rothwell, G.W., 1999. *Osmunda cinnamomea* (Osmundaceae) in the Upper Cretaceous of western North America: additional evidence for exceptional species longevity among filicalean ferns. Int. J. Plant Sci. 160, 425–433.

Sharpe, J.M., 1993. Plant growth and demography of the Neotropical herbaceous fern *Danaea wendlandii* (Marattiaceae) in a Costa Rican rain forest. Biotropica 25, 85–94.

Shen, H., Jin, D., Shu, J.-P., Zhou, X.-L., Lei, M., Wei, R., Shang, H., Wei, H.-J., Zhang, R., Liu, L. *et al.*, 2018. Large-scale phylogenomic analysis resolves a backbone phylogeny in ferns. GigaScience. 7, 1–11.

Siddall, M.E., 1996. Stratigraphic consistency and the shape of things. Syst. Biol. 45, 111–115.

Siddall, M.E., 1998. Stratigraphic fit to phylogenies: a proposed solution. Cladistics 14, 201–208.

Skog, J.E. and Banks, H.P., 1973. *Ibyka amphikoma*, gen. et sp. n., a new protoarticulate precursor from the late Middle Devonian of New York state. Am. J. Bot. 60, 366–380.

Smith, S.A., Beaulieu, J.M. and Donoghue, M.J., 2010. An uncorrelated relaxed-clock analysis suggests an earlier origin for flowering plants. Proc. Natl. Acad. Sci. USA 107, 5897–5902.

Soltis, P.S., Soltis, D.E., Savolainen, V., Crane, P.R. and Barraclough, T.G., 2002. Rate heterogeneity among lineages of tracheophytes: integration of molecular and fossil data and evidence for molecular living fossils. Proc. Natl. Acad. Sci. USA 99, 4430–4435.

Stamatakis, A., 2014. RAxML version 8: a tool for phylogenetic analysis and post-analysis of large phylogenies. Bioinformatics 30, 1312–1313.

Sterli, J., Pol, D. and Laurin, M., 2013. Incorporating phylogenetic uncertainty on phylogeny-based palaeontological dating and the timing of turtle diversification. Cladistics 29, 233–246.

Stevenson, D.W. and Loconte, H., 1996. Ordinal and familial relationships in pteridophyte genera. In: Camus, J.M., Gibby, M. and Johns, R.J. (Eds.) Pteridology in Perspective. Royal Botanic Gardens, Kew, pp. 435–467.

Stewart, W.N. and Rothwell, G.W., 1993. Paleobotany and the Evolution of Plants, 2nd edn. Cambridge University Press, Cambridge.

Stidd, B.M., 1974. Evolutionary trends in the Marattiales. Ann. Missouri Bot. Gard. 61, 388–407.

Stubblefield, S.P., 1984. Taxonomic delimitation among Pennsylvanian marattialean fructifications. J. Paleontol. 58, 793–803.

Suchard, M.A., Lemey, P., Baele, G., Ayres, D.L., Drummond, A.J. and Rambaut, A., 2018. Bayesian phylogenetic and phylodynamic data integration using BEAST 1.10. Virus. Evolution 4, vey016.

Tavares, T.M.V., Rohn, R., Rößler, R. and Noll, R., 2014. Petrified Marattiales pinnae from the Lower Permian of North-Western Gondwana (Parnaíba Basin, Brazil). Rev. Palaeobot. Palynol. 201, 12–28.

Taylor, T.N., 1967. On the structure and phylogenetic relationships of the fern *Radstockia* Kidston. Palaeontology 10, 43–46.

Testo, W. and Sundue, M., 2016. A 4000-species dataset provides new insight into the evolution of ferns. Mol. Phylogenet. Evol. 105, 200–211.

Thiel, T., Michalek, W., Varshney, R. and Graner, A., 2003. Exploiting EST databases for the development and characterization of gene-derived SSR-markers in barley (*Hordeum vulgare* L.). Theor. Appl. Genet. 106, 411–422.

Tuomisto, H., Kessler, M. and Smith, A.R., 2018. Prodromus of a fern flora for Bolivia. VIII. Marattiaceae. Phytotaxa 344, 64–68.

Vaidya, G., Lohman, D.J. and Meier, R., 2011. SequenceMatrix: concatenation software for the fast assembly of multi-gene datasets with character set and codon information. Cladistics 27, 171–180.

Van Cittert, J.H.A., 1966. Palaeobotany of the mesophytic II. New and noteworthy Jurassic ferns from Yorkshire. Acta Bot. Neerl. 15, 284–289.

Vera, E.I. and Césari, S.N., 2016. Marattiaceae synangia from the Lower Cretaceous of Antarctica. Rev. Palaeobot. Palynol. 235, 6–10.

Wagner, R.H., Hill, C.R. and El-Khayal, A.A., 1985. *Gemellitheca* gen. nov., a fertile pecopterid fern from the upper Permian of the Middle East. Scr. Geol. 79, 51–74.

Walker, J.D., Geissman, J.W., Bowring, S.A. and Babcock, L.E., 2018. Geologic Time Scale v. 5.0. Geological Society of America. https://doi.org/10.1130/2018.CTS005R3C

Wan, Z. and Basinger, J.F., 1992. On the fern *Pectinangium* Li et al., emend. (Marattiales), with spores in situ from the Permian of southern China. Rev. Palaeobot. Palynol. 75, 219–238.

Wang, H. and Guanxiu, Y., 1996. Microscopical study of *Qasimia* from the Permian of western Henan Province, Central China. The Palaeobotanist. 45, 255–258.

Wang, M. and Lloyd, G.T., 2016. Rates of morphological evolution are heterogeneous in Early Cretaceous birds. Proc. R. Soc. B Biol. Sci. 283, 20160214.

Wang, Q., Ablaev, A.G., Wang, Y.F. and Li, C.S., 2006. Paleocene Wuyun flora in Northeast China: *Woodwardia bureiensis*, *Dryopteris* sp. and *Osmunda sachalinensis*. Acta Phytotax. Sin. 44, 712–720.

Wang, S.-J., Hilton, J., He, X.-Y., Seyfullah, L.J. and Shao, L., 2014. The anatomically preserved stem *Zhongmingella* gen. nov. from the Upper Permian of China: evaluating the early evolution and phylogeny of the Osmundales. J. Syst. Palaeontol. 12, 1–22.

Wang, Y.D., 1999. Fertile organs and in situ spores of *Marattia asiatica* (Kawasaki) Harris (Marattiales) from the Lower Jurassic Hsiangchi Formation in Hubei, China. Rev. Palaeobot. Palynol. 107, 125–144.

Webb, J.A., 2001. A new marattialean fern from the Middle Triassic of Eastern Australia. Proc. Linn. Soc. N.S.W. 123, 215–224.

Wheeler, W., Aagesen, L., Arango, C.P., Faivovich, J., Grant, T., D'Haese, C., Janies, D., Smith, W.L., Varón, A. and Giribet, G., 2006. Dynamic Homology and Phylogenetic Systematics: A Unified Approach Using POY. American Museum of Natural History, New York.

Wickett, N.J., Mirarab, S., Nguyen, N., Warnow, T., Carpenter, E., Matasci, N., Ayyampalayam, S., Barker, M.S., Burleigh, J.G., Gitzendanner, M.A. *et al.*, 2014. Phylotranscriptomic analysis of the origin and early diversification of land plants. Proc. Natl Acad. Sci. USA 111, E4859–E4868.

Wikström, N. and Pryer, K.M., 2005. Incongruence between primary sequence data and the distribution of a mitochondrial atp1 group II intron among ferns and horsetails. Mol. Phylogenet. Evol. 36, 484–493.

Wikström, N., Kenrick, P. and Vogel, J.C., 2002. Schizaeaceae: a phylogenetic approach. Rev. Palaeobot. Palynol. 119, 35–50.

Wolf, P.G., Roper, J.M. and Duffy, A.M., 2010. The evolution of chloroplast genome structure in ferns. Genome 53, 731–738.

Wolf, P.G., Rowe, C.A., Sinclair, R.B. and Hasebe, M., 2003. Complete nucleotide sequence of the chloroplast genome from a leptosporangiate fern, *Adiantum capillus-veneris* L. DNA Res. 10, 59–65.

Wolf, P.G., Der, J.P., Duffy, A.M., Davidson, J.B., Grusz, A.L. and Pryer, K.M., 2011. The evolution of chloroplast genes and genomes in ferns. Plant Mol. Biol. 76, 251–261.

Wu, C.S., Wang, Y.N., Liu, S.M. and Chaw, S.M., 2007. Chloroplast genome (cpDNA) of *Cycas taitungensis* and 56 cp protein-coding genes of *Gnetum parvifolium*: insights into cpDNA evolution and phylogeny of extant seed plants. Mol. Biol. Evol. 24, 1366–1379.

Wyman, S.K., Jansen, R.K. and Boore, J.L., 2004. Automatic annotation of organellar genomes with DOGMA. Bioinformatics 20, 3252–3255.

Yang, S., Wang, J. and Pfefferkorn, H.W., 2008. *Marattia aganzhenensis* sp. nov. from the Lower Jurassic Daxigou Formation of Lanzhou, Gansu, China. Int. J. Plant Sci. 169, 473–482.

Yin, T., Cook, D. and Lawrence, M., 2012. ggbio: an R package for extending the grammar of graphics for genomic data. Genome Biol., 13, R77.

Zerbino, D.R. and Birney, E., 2008. Velvet: algorithms for de novo short read assembly using de Bruijn graphs. Genome Res. 18, 821–829.

Zhifeng, G. and Thomas, B.A., 1993. A new fern from the lower Permian of China and its bearing on the evolution of the marattialeans. Palaeontology 36, 81–89.

Zhu, A., Guo, W., Gupta, S., Fan, W. and Mower, J.P., 2015. Evolutionary dynamics of the plastid inverted repeat: the effects of expansion, contraction, and loss on substitution rates. New Phytol. 209, 1747–1756.

Zodrow, E.L., Šimůnek, Z., Cleal, C.J., Bek, J. and Pšenička, J., 2006. Taxonomic revision of the Palaeozoic marattialean fern *Acitheca* Schimper. Rev. Palaeobot. Palynol. 138, 239–280.

Supporting Information

Additional supporting information may be found online in the Supporting Information section at the end of the article.

Figure S1. Plastome coverage and gene track visualization of the sequenced plastomes. Plastome coverage was evaluated by remapping the corresponding reads to the plastomes, and gene tracks were derived from the corresponding GFF files.

Figure S2. Maps of the newly generated plastomes.

Table S1. Gene-wise alignment statistics and informative sites per gene alignment in the plastome analysis of the ferns with seed plant outgroups.

Appendix S1. Data partitioning and evolutionary models in the Bayesian analyses.

Appendix S2. Biogeographical connectivity matrices through time.

Appendix 1

Taxa investigated with literature references and herbarium specimens studied for the character coding.

Acaulangium bulbaceum (Graham) Millay. Mamay (1950), Millay (1977, 1997), Lesnikowska (1989), Stubblefield (1984). *Acitheca adaensis* Mapes & Schabilion. Mapes and Schabilion (1979a), Zodrow et al. (2006). *Acitheca polymorpha* (Brongniart) Schimper. Lesnikowska and Galtier (1991), Millay (1997), Zodrow et al. (2006). *Angiopteris angustifolia* C.Presl. Murdock (2008b). *Christenhusz K 03 640030 08088* (TUR). *Angiopteris blackii* Van Konijnenburg-van Cittert. Hill (1987). *Angiopteris evecta* (G.Forst.) Hoffm. Hill and Camus (1986a), Rolleri (2002), Murdock (2008b). *Christenhusz et al. 2992* (TUR), *Christenhusz et al. 3111* (TUR), *Christenhusz et al. 3166* (TUR), *Christenhusz et al. 3292* (TUR), *Christenhusz et al. 5100* (TUR), *Christenhusz et al. 5133* (TUR). *Araiangium pygmaeum* (Graham) Millay. Millay (1982, 1997). *Buritiranopteris costata* Tavares, Rohn, Rößler & Noll. Tavares et al. (2014). *Christensenia aesculifolia* (Blume) Maxon. Hill and Camus (1986a), Rolleri (1993), Rolleri et al. (1996), Murdock (2008a; 2008b). *Danaea sellowiana* C.Presl. Hill and Camus (1986a). *Christenhusz 4940* (TUR), *Christenhusz 4944* (TUR), *Mynssen 1074* (TUR). *Danaeites rigida* Gu & Zhi. Liu et al. (2001). *Danaeopsis fecunda* Halle.

Kustatscher et al. (2012). *Danaeopsis marantacea* Webb. Webb (2001). *Eoangiopteris andrewsii* Mamay. Lesnikowska (1989), Millay (1997). *Eoangiopteris goodii* Millay. Millay (1978, 1997). *Eupodium cicutifolium* (Kaulf.) Lehtonen. del Carmen Lavalle (2003, 2007), del Carmen Lavalle et al. (2011). *Christenhusz et al. 4780* (TUR), *Christenhusz et al. 4781* (TUR). *Eupodium kaulfussii* (J.Sm.) J.Sm. Hill and Camus (1986a), del Carmen Lavalle (2003, 2007), Murdock (2008a), Christenhusz (2010), del Carmen Lavalle et al. (2011). *Christenhusz et al. 3266* (TUR), *Christenhusz et al. 4788* (TUR), *Lehtonen et al. 571* (TUR). *Gemellitheca saudica* Wagner, Hill & El-Khayal. Wagner et al. (1985). *Grandeuryella renaultii* (Stur) Weiss. Lesnikowska and Galtier (1992), Millay (1997). *Marantoidea acara* Webb. Webb (2001). *Marattia laxa* Kunze. del Carmen Lavalle (2003, 2007), Murdock (2008b), del Carmen Lavalle et al. (2011). *Christenhusz et al. 1313* (TUR), *Christenhusz et al. 3272* (TUR), *Tuomisto et al. 17511* (TUR). *Marattiopsis aganzhenensis* (Yang et al.) Escapa et al. Yang et al. (2008). *Marattiopsis anglica* Thomas. (Van Cittert, 1966), van Konijnenburg-van Cittert (1975) Harris (1961). *Marattiopsis asiatica* Kawasaki. Wang (1999). *Marattiopsis patagonica* Escapa et al. Escapa et al. (2014). *Marattiopsis vodrazkae* Kvaček. Kvaček (2014). *Millaya tularosana* Mapes & Schabilion. Mapes and Schabilion (1979b). *Osmundastrum cinnamomeum* (L.) C.Presl. Miller (1971), Jud et al. (2008), Wang et al. (2014), Bomfleur et al. (2017). *Brisson 76095* (TUR), *Hamel & Brisson 14449* (TUR), *Eiten 1294* (TUR), *Guay et al. s.n.* (TUR). *Pectinangium lanceolatum* Li et al. Wan and Basinger (1992). *Ptisana novoguineensis* (Rosenst.) Murdock. Rosenstock (1912). *Qasimia lanceolata* Wang & Yang. Wang and Guanxiu (1996). *Qasimia schyfsmae* (Lemoigne) Hill, Wagner & El-Khayal. Hill et al. (1985). *Radstockia kidstonii* Taylor. Taylor (1967). *Scolecopteris antarctica* Delevoryas et al. Delevoryas et al. (1992). *Scolecopteris calicifolia* Millay. Millay (1979, 1997), Lesnikowska (1989). *Scolecopteris globiforma* Millay & Galtier. Millay and Galtier (1990). *Scolecopteris gnoma* Lesnikowska & Millay. Lesnikowska (1989). *Scolecopteris illinoensis* Ewart. Millay (1979), Lesnikowska (1989). *Scolecopteris latifolia* Graham. Mamay (1950), Millay (1979, 1997), Lesnikowska (1989). *Scolecopteris majopsis* Millay. Millay (1979), Lesnikowska (1989). *Scolecopteris mamayi* Millay. Millay (1979), Lesnikowska (1989). *Scolecopteris minor* Hoskins. Mamay (1950), Millay (1979, 1997), Lesnikowska (1989). *Sydneia manleyi* Pšenička. Pšenička et al. (2003, 2014). *Taiyuanitheca tetralinea* Gao & Thomas. Zhifeng and Thomas (1993). *Zhutheca densata* (Gu & Zhi) Liu, Li & Hilton. Liu et al. (2000b).

Appendix 2

Phenotypic character descriptions and argumentation.

0. Root pith sclerified: (0) no; (1) yes. Similar to Hill and Camus (1986a), char. 12; Pryer et al. (1995), char. 21; Rothwell (1999), char. 48; Murdock (2008b), char. 1; Rothwell et al. (2018), char. 6. Uninformative in the current matrix.

1. Continuous band of sclerenchymatous fibres in cortex of root: (0) absent; (1) present. Similar to Hill and Camus (1986a), char. 13; Murdock (2008b), char. 2; Rothwell et al. (2018), char. 7.

2. Root hairs: (0) absent; (1) present. Similar to Stevenson and Loconte (1996), char. 3; Jud et al. (2008), char. 1267; Schneider et al. (2009), char. 41.

3. Root hair structure: (0) unicellular; (1) multicellular. Similar to Hill and Camus (1986a), char. 15; Stevenson and Loconte (1996), char. 3; Schneider et al. (2009), char. 42; Rothwell et al. (2018), char. 9. Uninformative in the current matrix.

4. Root anatomy: (0) diarch; (1) polyarch. Similar to Rothwell (1999), char. 16; Pryer et al. (1995), char. 35; Schneider et al. (2009), char. 45; Rothwell et al. (2018), char. 8. Uninformative in the current matrix.

5. Outer root cortex: (0) sclerenchymatous; (1) parenchymatous. Similar to Pryer et al. (1995), char. 94; Schneider et al. (2009), char. 48. Uninformative in the current matrix.

6. Root mantle: (0) absent; (1) present. Similar to Rothwell et al. (2018), char. 4.

7. Stem symmetry: (0) radial; (1) dorsiventral. Similar to Hill and Camus (1986a), chars. 17 and 19; Pryer et al. (1995), char. 26; Stevenson and Loconte (1996), char. 8; Rothwell (1999), char. 5; Murdock (2008b), char. 3; Jud et al. (2008), char. 1228; Schneider et al. (2009), char. 25; Rothwell et al. (2018), chars. 1 and 12.

8. Stem shape: (0) elongate; (1) squat. Similar to Hill and Camus (1986a), char. 18; Rothwell et al. (2018), char. 2.

9. Stem sclerenchyma: (0) absent; (1) present. Similar to Hill and Camus (1986a), chars. 11 and 14; Schneider et al. (2009), char. 32; Wang et al. (2014), char. 15; Rothwell et al. (2018), char. 18.

10. Mature shoot stele type: (0) ectophloic; (1) siphonostele; (2) dictyostele. Similar to Hill and Camus (1986a) chars. 1–4; Pryer et al. (1995), char. 27; Stevenson and Loconte (1996), char. 19; Rothwell (1999), chars. 27–39; Jud et al. (2008), char. 1232–1233; Schneider et al. (2009), char. 26; Wang et al. (2014), char. 3 and 10; Rothwell et al. (2018), char. 14.

11. Vascular stele cycles: (0) monocyclic; (1) polycyclic. Similar to Hill and Camus (1986a), char. 2; Pryer et al. (1995), char. 28; Rothwell (1999), char. 34; Schneider et al. (2009), char. 27; Rothwell et al. (2018), char. 16.

12. Pneumathodes: (0) absent; (1) scattered all around petiole. Similar to Schneider et al. (2009), char. 13. Uninformative in the current matrix.

13. Petiole stele number: (0) monostele; (1) polystele. Similar to Pryer et al. (1995), char. 23; Stevenson and Loconte (1996), char. 40; Rothwell (1999), char. 40; Schneider et al. (2009), char. 18.

14. Xylem configuration in petiole: (0) horseshoe-shape variation; (1) polycyclic. Similar to Hill and Camus (1986a), char. 3; Pryer et al. (1995), char. 24; Rothwell (1999), chars. 41 and 43–46; Schneider et al. (2009), char. 19.

15. Pitting pattern of metaxylem: (0) multiseriate scalariform; (1) scalariform. Similar to Pryer et al. (1995), char. 25; Stevenson and Loconte (1996), char. 17; Rothwell (1999), chars. 37–38; Schneider et al. (2009), char. 53. Uninformative in the current matrix.

16. Scales: (0) absent; (1) present. Similar to Hill and Camus (1986a), char 44; Pryer et al. (1995), char. 31; Stevenson and Loconte (1996), char. 43; Rothwell (1999), chars. 23–24; Liu et al. (2000a), char. 6; Schneider et al. (2009), char. 30; Rothwell et al. (2018), char. 61. Uninformative in the current matrix.

17. Scale cells: (0) isodiametric; (1) elongate. Similar to Hill and Camus (1986a), char. 40; Murdock (2008b), char. 27; Rothwell et al. (2018), char. 40.

18. Peltate laminar scales: (0) with centrally attached stalks; (1) strongly asymmetrical. Similar to Murdock (2008b), char. 28; Rothwell et al. (2018), char. 42.

19. Mucilage canals: (0) absent; (1) present. Similar to Hill and Camus (1986a), chars. 7–10; Pryer et al. (1995), char. 37; Stevenson and Loconte (1996), char. 14; Schneider et al. (2009), char. 58; Rothwell et al. (2018), char. 22. Uninformative in the current matrix.

20. Fertile-sterile leaf differentiation: (0) monomorphic; (1) dimorphic. Similar to Hill and Camus (1986a), char. 47; Pryer et al. (1995), char. 2; Stevenson and Loconte (1996), char. 42; Rothwell (1999), char. 57; Murdock (2008b), char. 11; Schneider et al. (2009), char. 4; Liu et al. (2000a), char. 10; Murdock (2008b), char. 11; Schneider et al. (2009), char. 4; Rothwell et al. (2018), char. 54.

21. Fertile fronds: (0) almost without lamina; (1) with lamina. Similar to Wang et al. (2014), char. 27.

22. Blade dissection: (0) once pinnate; (1) twice pinnate; (2) more than twice pinnate. Similar to Hill and Camus (1986a), chars. 20-23; Pryer et al. (1995), char. 3; Stevenson and Loconte (1996), char. 20; Liu et al. (2000a), char. 2; Murdock (2008b), chars. 8–9; Schneider et al. (2009), char. 5; Wang et al. (2014), char. 25; Rothwell et al. (2018), char. 30.

23. Basal pinnae more elaborated: (0) no; (1) yes. Similar to Murdock (2008b), char. 12; Rothwell et al. (2018), char. 13.

24. Ultimate pinnule size: (0) ≤1.5 cm; (1) 1.5–4 cm; (2) >4 cm.

25. Rachis wings: (0) absent; (1) present.

26. Number of fronds produced at a time: (0) multiple; (1) typically only one. Similar to Murdock (2008b), char. 14; Rothwell et al. (2018), char. 28. Uninformative in the current matrix.

27. Pinnule attachment: (0) attached to midrib by entire base; (1) attached to midrib by single point. Similar to Liu et al. (2000a), char. 3; Cleal (2015), char. 3.

28. Pinnule base: (0) rounded; (1) auriculate cordate acute. Similar to Rothwell et al. (2018), char. 31.

29. Pinnule apices: (0) rounded; (1) tapered. Similar to Murdock (2008b), char. 17; Rothwell et al. (2018), char. 32.

30. Fertile pinnules: (0) not reflexed; (1) reflexed to protect the sori. Similar to Hill and Camus (1986a), char. 38; Rothwell et al. (2018), char. 59.

31. Reflexed margin completely envelopes the sporangia: (0) no; (1) yes. Similar to Rothwell et al. (2018), char. 62.

32. Lamina margins of pinnae or pinnules excluding apex: (0) dentate; (1) entire; (2) lobed (multiple ends of bifurcating vein); (3) decompound with cuneate segments; (4) incised, Similar to Hill and Camus (1986a), char. 37; Liu et al. (2000a), char. 7; Rothwell et al. (2018), char. 60.

33. Abaxial multicellular hairs: (0) absent; (1) present. Similar to Hill and Camus (1986a), char. 44; Liu et al. (2000a), char. 5; Rothwell et al. (2018), char. 61.

34. Forking of veins in fertile frond: (0) mainly simple; (1) normally forking near the midrib; (2) forking in the lamina; (3) irregular. Similar to Liu et al. (2000a), char. 4; Murdock (2008b), char. 35

35. Veins: (0) free; (1) anastomosing with free included veinlets; (2) anastomosing without free included veinlets. Similar to Hill and Camus (1986a), chars. 45–46; Pryer et al. (1995), char. 7; Stevenson and Loconte (1996), char. 38; Rothwell (1999), char. 22; Liu et al. (2000a), char. 4; Murdock (2008b), char. 34; Schneider et al. (2009), char. 10; Rothwell et al. (2018), char. 50.

36. Vein density: (0) <7 per cm; (1) 9–16 per cm; (2) >30 per cm. Similar to Rothwell et al. (2018), char. 105.

37. False veins: (0) absent; (1) present. Similar to Hill and Camus (1986a), char. 39; Murdock (2008b), char. 33; Rothwell et al. (2018), char. 51.

38. Pulvini: (0) absent; (1) present. Similar to Hill and Camus (1986a), chars. 6 and 26–28; Pryer et al. (1995), char. 15; Stevenson and Loconte (1996), char. 32; Murdock (2008b), chars. 4–7; Schneider et al. (2009), char. 12; Rothwell et al. (2018), chars. 109–113.

39. Soft spines on veins: (0) absent; (1) present. Similar to Hill and Camus (1986a), char. 25; Liu et al. (2000a), char. 8; Murdock (2008b), char. 22; Rothwell et al. (2018) 52. Uninformative in the current matrix.

40. Sutures at pinnule bases: (0) absent; (1) present. Based on Murdock (2008a). The extant members of *Ptisana* typically have sutures at pinnule bases (Murdock, 2008a) and, because some of the fossil species are always preserved as detached pinnules, it has been suggested that they also had sutures (Escapa et al., 2014; Kvaček, 2014). However, in the lack of clear evidence these fossils were here coded as having unknown state. Uninformative in the current matrix.

41. Stipules: (0) absent; (1) present. Similar to Hill and Camus (1986a), char. 5; Pryer et al. (1995), char. 89; Rothwell (1999), char. 26. The extant Marattiales have large flap-like organs attached in a pair at the bases of rachises (Hill and Camus, 1986a). Osmundalean ferns often have sheathing structures called stipules at their rachis bases, but these structures are not considered homologous with the marattialean stipules.

42. Stomatal type: (0) anomocytic; (1) cyclocytic. Similar to Hill and Camus (1986a), char. 31; Pryer et al. (1995), char. 12; Stevenson and Loconte (1996), char. 35; Liu et al. (2000a), char. 9; Schneider et al. (2009), char. 56; Rothwell et al. (2018), char. 114.

43. Stomatal shape: (0) elliptical; (1) circular. Similar to Murdock (2008b), char. 19; Rothwell et al. (2018), char. 116. Uninformative in the current matrix.

44. Stomatal guard cells: (0) functional; (1) permanently open. Similar to Hill and Camus (1986a), char. 30; Murdock (2008b), char. 18; Rothwell et al. (2018), char. 115. Uninformative in the current matrix.

45. Stomatal complex: (0) surficial or slightly sunken; (1) raised. Similar to Murdock (2008b), char. 20; Rothwell et al. (2018), char. 117.

46. Idioblasts in abaxial epidermis: (0) absent; (1) present. Similar to Hill and Camus (1986a), char. 36; Murdock (2008b), char. 23; Rothwell et al. (2018), char. 35.

47. Laminar idioblast groupings: (0) solitary or small clusters; (1) dense areas of idioblasts. Similar to Murdock (2008b), char. 24; Rothwell et al. (2018), char. 36.

48. Laminar tissue expanded between sori/sporangia: (0) absent; (1) present. Similar to Hill and Camus (1986a), char. 50; Liu et al. (2000a), char. 15; Murdock (2008b), char. 10; Rothwell et al. (2018), char. 55.

49. Sporangial grouping: (0) absent; (1) present. Similar to Pryer et al. (1995), char. 47; Rothwell (1999), char. 65; Schneider et al. (2009), char. 59.

50. Sporangial stalk width: (0) four to six cell rows wide; (1) more than six cell rows. Similar to Pryer et al. (1995), char. 45; Stevenson and Loconte (1996), char. 63; Rothwell (1999), char. 71; Schneider et al. (2009), char. 74. Uninformative in the current matrix.

51. Sporangial development: (0) eusporangiate; (1) leptosporangiate. Similar to Pryer et al. (1995), char. 42; Stevenson and Loconte (1996), char. 48; Rothwell (1999), chars. 73 and 79; Schneider et al. (2009), char. 72. Uninformative in the current matrix.

52. Annulus: (0) absent; (1) present. Similar to Pryer et al. (1995), char. 56; Stevenson and Loconte (1996), char. 64; Rothwell (1999), char. 74; Liu et al. (2000a), char. 21; Schneider et al. (2009), char. 76; Rothwell et al. (2018), char. 63. Uninformative in the current matrix.

53. Shape of sporangia: (0) elongate; (1) ovoid; (2) obovoid; (3) globular. Similar to Cleal (2015), char. 4.

54. Sporangial aperture development: (0) apertures develop longitudinally; (1) apertures develop apically; (2) apertures develop vertically. Similar to Hill and Camus (1986a), char. 69; Liu et al. (2000a), char. 19; Murdock (2008b), char. 45; Rothwell et al. (2018), char. 88.

55. Sporangial aperture shape: (0) slit; (1) pore. Similar to Hill and Camus (1986a), char. 69; Liu et al. (2000a), char. 19; Murdock (2008b), char. 44; Rothwell et al. (2018), char. 87. Uninformative in the current matrix.

56. Sporangial tips: (0) absent; (1) present. Similar to Liu et al. (2000a), char. 23; Murdock (2008b), char. 49; Rothwell et al. (2018), char. 83.

57. Sporangial tip length: (0) short; (1) long. Similar to Rothwell et al. (2018), char. 84.

58. Size of sporangia: (0) <1 mm; (1) >1 mm. Similar to Rothwell et al. (2018), char. 80.

59. Sporangia dorsal wall thickness: (0) one to two cells; (1) three or more cells. Similar to Liu et al. (2000a), char. 22; Rothwell et al. (2018), char. 82.

60. Indument borne on sporangia: (0) absent; (1) present. Similar to Hill and Camus (1986a), char. 49; Murdock (2008b), char. 29; Rothwell et al. (2018), char. 43.

61. Paraphyses: (0) absent; (1) present. Similar to Hill and Camus (1986a), char. 48; Murdock (2008b), char. 30; Rothwell et al. (2018), char. 44.

62. Sporangial outer wall cells: (0) isodiametric, rounded; (1) elongate, polygonal. Similar to Hill and Camus (1986a), char. 60; Murdock (2008b), char. 47.

63. Number of sporangia per synangium: (0) typically fewer than six; (1) typically 6–11; (2) typically 11–24; (3) ≤80. Similar to Hill and Camus (1986a), char. 63; Pryer et al. (1995), char. 51; Rothwell (1999), char. 67; Liu et al. (2000a), char. 24; Schneider et al. (2009), char. 63; Cleal (2015), char. 5; Rothwell et al. (2018), char. 69.

64. Sporangial fusion in synangia: (0) basally fused; (1) fused until opening in dehiscence; (2) fused but opening as two valves; (3) completely fused. Similar to Hill and Camus (1986a), chars. 59–60 and 64–68; Pryer et al. (1995), char. 83; Stevenson and Loconte (1996), char. 51; Rothwell (1999), char. 66; Liu et al. (2000a), char. 20; Murdock (2008b), chars. 42–43; Schneider et al. (2009), char. 69; Rothwell et al. (2018), chars. 66, 85–86 and 102.

65. Synangial division between valves: (0) deeply cut; (1) shallowly cut. Similar to Murdock (2008b) char. 46; Rothwell et al. (2018), char. 67.

66. Position of the synangia: (0) near to margin; (1) between the margin and the midrib. Similar to Hill and Camus (1986a), char. 57; Liu et al. (2000a), char. 16; Rothwell et al. (2018), char. 103.

67. Distribution of synangia: (0) single row; (1) two or more rows; (2) scattered. Similar to Hill and Camus (1986a), chars. 55–56; Liu et al. (2000a), char. 17; Murdock (2008b), char. 38.

68. Symmetry of synangia: (0) radial; (1) bilateral. Similar to Hill and Camus (1986a), char. 58; Liu et al. (2000a), char. 11; Murdock (2008b), char. 37; Rothwell et al. (2018), char. 70.

69. Receptacle: (0) flat or slightly raised; (1) developed into a stalk. Similar to Hill and Camus (1986a), char. 53; Pryer et al. (1995), char. 43; Stevenson and Loconte (1996), char. 60; Liu et al. (2000a), char. 12; Murdock (2008b), char. 48; Schneider et al. (2009), char. 70; Cleal (2015), char. 6; Rothwell et al. (2018), char. 74.

70. Tracheids in placental tissue: (0) absent; (1) present. Similar to Hill and Camus (1986a), char. 51; Liu et al. (2000a), char. 13; Murdock (2008b), char. 36; Rothwell et al. (2018), char. 79.

71. Sporangia/synangia: (0) pendant; (1) lying transversely across the lamina. Based on Wagner et al. (1985).

72. Spore output per sporangium: (0) a few hundred; (1) a thousand or more. Similar to Pryer et al. (1995), char. 46; Stevenson and Loconte (1996), char. 67; Rothwell (1999), char. 78; Schneider et al. (2009), char. 75; Wang et al. (2014), char. 26.

73. Spore morphology: (0) monolete; (1) trilete; (2) alete. Similar to Hill and Camus (1986a), char. 70; Pryer et al. (1995), char. 60; Stevenson and Loconte (1996), char. 71; Rothwell (1999), char. 86; Liu et al. (2000a), char. 26; Murdock (2008b), char. 50; Schneider et al. (2009), char. 84; Cleal (2015), char. 8; Rothwell et al. (2018), char. 92.

74. Exine ornamentation: (0) smooth; (1) granular; (2) echinate; (3) echinate perispore on tubercles. Similar to Hill and Camus (1986a), chars. 71–73; Pryer et al. (1995), char. 66; Stevenson and Loconte (1996), char. 81; Rothwell (1999), char. 88; Liu et al. (2000a), char. 27; Murdock (2008b), chars. 51–53; Schneider et al. (2009), char. 91; Cleal (2015), char. 7; Rothwell et al. (2018), char. 97.

75. Spore size: (0) >40 μm; (1) <40 μm. Similar to Liu et al. (2000a), char. 25; Rothwell et al. (2018), char. 91.

76. Spores chlorophyllous: (0) no; (1) yes. Similar to Pryer et al. (1995), char. 61; Stevenson and Loconte (1996), char. 69; Schneider et al. (2009), char. 97. Uninformative in the current matrix.

Appendix 3

Phenotypic character data matrix. Polymorphisms are marked by letters as follows: a = [0 1], b = [1 2], c = [0 1 2]. Dashes indicate inapplicable states, question marks indicate unknown states.

```
Osmundastrum cinnamomeum-?100000010000000-010001000-00-102010000000000-000113200-00001————001001
Angiopteris evecta0011110010111111111101102001010-0010111001100111011002000-0101120-00100011110
Angiopteris angustifolia0011110010111111111101102001010-0010111001100111011002000-0101120-00100011110
Christensenia aesculifolia0011110100101111100101002-01010-103110100111110-011001100-0101013-12001010210
Danaea sellowiana1111110101111111100110002001010-101010100110000-111001110-0000133-1c100010210
Eupodium kaulfussii0011110010111111111101211111310-0010001101100010011001001001000121101110210
Ptisana novoguineensis0011110010111111111101102101010-0000101011100010011001001001010022000100010110
Marattia cicutifolia0011110010111111111101102101010-0010101001100010011001001001010022010111010210
Marattia laxa0011110010111111111101112101010-0020111001100010011001001101010221001000010110
Marattiopsis aganzhenensis??????????????????????011?2??1010-101010?0?????????011001000010??32?0010?00011?
Marattiopsis asiatica??????????????????????011?20?11?0-101011?00??????011001000010?030-0010?01a11?
Marattiopsis anglica??????????????????????011?20?10?0-101011?0??????011001000?010?032?0010?0?a11?
Marattiopsis vodrazkae??????????????????????01??1??110-001010?0??????011001001010?11201011?0?011?
Marattiopsis patagonica??????????????????????01??2??1110-001011?0??????0110010010010?03200010?0?????
Angiopteris blackii??????????????????????011?21?1010-001010?00??????011002000-010?120-0010?01111?
Qasimia schyfsmae??????????????????????11b?b0?a200-102021?00?a0?0??011000000-1???13201010?0?021?
Qasimia lanceolata??????????????????????1b?20?1200-10202??00??????011000000-0????3201010?0?010?
Scolecopteris minor010-11100111?0011??1012?0000-0114000?0000010?0??011000011011?101-100110?001?
Scolecopteris majopsis010-11100111?001????012?0000-010100000000010?0??011000010111?101-100100?100?
Scolecopteris illinoensis010-11100111?001???1012?0000-0100000?0000010?0??011000001001??101-100110?001?
Acaulangium bulbaceum010-11100111?001????012?0000-010100000001?????0110010011010?101-100010?201?
Scolecopteris latifolia010-11100111?001???1112?0000-0114100000000010?0??011000001011?101-100100?101?
Scolecopteris mamayi010-11100111?0011??1112?0000-011410010000010?0??011000010101?101-100110?001?
Scolecopteris antarctica??????????????????????012?0000-011??????????????011000001?111?101-100110?201?
Scolecopteris globiforma????????1?????????012?0000-011?000?0000010?0??011000001?111?101-100100?001?
Scolecopteris calicifolia010-11100111?001???1112?0000-0114100?0000010?0??011000001?10??101-100100?001?
Scolecopteris gnoma010-11000111?0011??1112?0000-0114000?0000010?0??011000011001?101-100110?001?
Eoangiopteris goodii?10-11?00111???????012?0000-010101010000010?0??011000001110??121-101000?100?
Eoangiopteris andrewsii?10-11?00111???????012?0000-010101010000010?0??011000001000???21-1010000100?
Acitheca polymorpha?10-11100111?001????01200000-010102020000010?0??011000011101??01-1000?0?100?
Acitheca adaensis???????????????????012?0000-011401010?00??????011000000111a1?101-100010?1?0?
Millaya tularosana??????????????????????1??0000-00-100010?00??????111000000-1?0?121-101010??10?
Danaeites rigida??????????????????????1b?0??0-00-100010?00??????011000000-100?121-1010?0?111?
Radstockia kidstonii??????????????????????02?0??a-?-300000?00??????01100??0-0????21-0010?0?100?
Sydneia manleyi??????????????????????102?0??a-?-301000?00??0?0??011000000-0???121-0010?0?a01?
Zhutheca densata??????????????????????12?0??0-00-201020?00??????011000100????01-110??01001?
Taiyuanitheca tetralinea??????????????????????012?0??0-0101010?0?00??????01100?000-0?0??21-1100?0?????
Grandeuryella renaultii??????????????????????012?0??0-010101010?00??????011000001000?111-101011?001?
Araiangium pygmaeum?????????????????1???112?0??0-00-1000?0?00??????011000010001?101-100000?100?
Buritiranopteris costata?10-11100110?101?????12?0000-0114010b00000?????011000000-1?0??01-1000?011?1?
Danaeopsis fecunda??????????????????????110?20?1010-101210?00??????001000000-0????————01100?
Danaeopsis marantacea??????????????????????110?20?1000-101210?00??????001000000-0????————01100?
Marantoidea acara??????????????????????110?20?a010-101210?00??????001000000-0????———?0?????
Pectinangium lanceolatum??????????????????????01b?20?0-010101010?00??????011000??0-110??0??1010?0?1?0?
Gemellitheca saudica?????????????????1???112?0??0-011101020?00?00?0??011000000-1???101-0010?11b01?
```